K/PS--1187

DE87 008955

GAS-PHASE THERMAL DISSOCIATION OF URANIUM HEXAFLUORIDE: INVESTIGATION BY THE TECHNIQUE OF LASER-POWERED HOMOGENEOUS PYROLYSIS

W. D. Bostick

Process Support Division
Oak Ridge Gaseous Diffusion Plant

W. H. McCulla

Los Alamos National Laboratory
Los Alamos, New Mexico 87545

L. D. Trowbridge

Engineering Physics and Mathematics Division
Oak Ridge National Laboratory

April 1987

Prepared by the
OAK RIDGE GASEOUS DIFFUSION PLANT
Oak Ridge, Tennessee 37831
operated by
MARTIN MARIETTA ENERGY SYSTEMS, INC.
for the
U.S. Department of Energy
under Contract No. DE-AC05-84OR21400

DISCLAIMER

CONTENTS

LIST OF FIGURES

LIST OF FIGURES (Continued)

LIST OF TABLES

SUMMARY

In the gas-phase, uranium hexafluoride decomposes thermally in a quasi-unimolecular reaction to yield uranium pentafluoride and atomic fluorine:

$$UF_6 \xrightarrow{k_u} UF_5 + F \ .$$

We have investigated this reaction using the relatively new technique of laser-powered homogeneous pyrolysis, in which a megawatt infrared laser is used to generate short pulses of high gas temperatures under strictly homogeneous conditions. In our investigation, SiF_4 is used as the sensitizer to absorb energy from a pulsed CO_2 laser and to transfer this energy by collisions with the reactant gas. Ethyl chloride is used as an external standard "thermometer" gas to permit estimation of the unimolecular reaction rate constants by a relative rate approach. When UF_6 is the reactant, CF_3Cl is used as reagent to trap atomic fluorine reaction product, forming CF_4 as a stable indicator which is easily detected by infrared spectroscopy:

$$CF_3Cl + F \rightarrow CF_4 + Cl \ .$$

Using these techniques, we estimate the UF_6 unimolecular reaction rate constant near the high-pressure limit:

$$k_\infty = 1.1 \times 10^{16} \exp[-(71.3 \pm 4) \quad \text{kcal mol}^{-1}/RT] \ s^{-1} \ .$$

This rate expression agrees with that derived by Schug and Wagner (1977) using the shock tube technique:

$$k_\infty = 3.3 \times 10^{16} \exp[-(70.3 \pm 4) \quad \text{kcal mol}^{-1}/RT] \ s^{-1} \ .$$

In the Appendix, we describe a computer program, written for the IBM PC, which predicts unimolecular rate constants based on the Rice-Ramsperger-Kassel theory. Parameterization of the theoretical model is discussed, and recommendations are made for "appropriate" input parameters for use in predicting the gas-phase unimolecular reaction rate for UF_6 as a function of temperature and gas composition and total pressure.

INTRODUCTION

Uranium hexafluoride (UF_6) is used in large quantities in the gaseous diffusion and gas centrifuge uranium enrichment enterprises, where its relative volatility (sublimation at 56.5°C) and thermal stability make it suitable for this application [Bacher and Jacob (1982)]. It is thus a key intermediate in the production of other uranium compounds for nuclear fuel processing.

The present investigation seeks to better define the thermal dissociation rate of UF_6, which proceeds in the gas phase by unimolecular decay [Schug and Wagner (1977)]:

$$UF_6 \underset{k_{r1}}{\overset{k_{u1}}{\rightleftarrows}} UF_5 + F \quad (\Delta H_{298} = +69.2 \text{ kcal/mol}) \ . \qquad (1)$$

(The parenthetic term, ΔH_{298}, represents the net enthalpy change at 298 K for the forward reaction. A positive value of ΔH_{298} indicates an endothermic reaction, whereas a negative value represents an exothermic reaction. Thermodynamic values used to compute ΔH_{298} in this work are taken from the National Bureau of Standards compilation of Wagman et al., 1982. Unless indicated otherwise, all reactants and products are assumed to be in the gas phase). The symbol "k" denotes the reaction rate constant, the temperature dependence of which is conventionally summarized in the form of an Arrhenius equation, i.e.,

$$k = A \exp(-E_a/RT) \ , \qquad (2)$$

where the term A is the so-called pre-exponential factor, E_a is the energy of activation, and R is the gas constant (1.987 cal deg-1 mol^{-1}).

The thermodynamic stability of UF_6 has long been recognized [see Tumanov (1968), Galkin and Tumanov (1971), Hassan and Deese (1974), Lau and Hildenbrand (1982), Leitnaker (1983)], but, until recently, little was known about the unimolecular decay kinetics. This is due largely to the difficulties in handling UF_6 at elevated temperatures. Uranium hexafluoride is a strong oxidizing and fluorination agent and tends to react with hot container surfaces, i.e.,

$$UF_6 + M \xrightarrow{k_s} UF_{(6-n)} + MF_n \ , \qquad (3)$$

where M in Eq. (3) is any oxidizable material. The heterogeneous reaction [Eq. (3)] may predominate over the homogeneous reaction [Eq. (1)], which, together with the effects of recombination, makes it very difficult to assess the true unimolecular rate constant [Eq. (1)] using conventional measurement techniques.

A BRIEF INTRODUCTION TO UNIMOLECULAR REACTIONS

As previously indicated, thermal dissociation of UF_6 in the gas phase is believed to be a pseudounimolecular reaction. The unique properties of unimolecular reactions and some procedures used to model and predict their reaction rates are described in several standard texts and reviews [see Kassel (1932), Laidler (1965), Robinson and Holbrook (1972), Mulcahy (1973), and Troe (1975)].

In a unimolecular reaction, the activated complex is a single reactant which has gained the necessary energy of activation by collisions with other molecules [Laidler (1965)]. The reaction may be an isomerization or a decomposition. In general, the process may be represented as follows:

$$A + M \underset{k_{-4}}{\overset{k_4}{\rightleftarrows}} A^* + M \ , \tag{4}$$

$$A^* \xrightarrow{k_5} \text{products} \ , \tag{5}$$

where A* represents an energized molecule, and M represents a collision partner which transfers energy. At high gas pressures (high collision rate), the reaction of the energized molecule is rate limiting, and the empirical rate expression is first order with respect to the reacting species; as the pressure is decreased, the concentration dependence gradually changes to second order (i.e., the rate of activation by collision with species M becomes the rate-limiting step).

Many subtle theoretical formulations have been proposed to model and predict the pressure-dependent "fall-off" of k_u. A useful treatment is known as the Rice-Ramsperger-Kassel theory, described in the Appendix.

PREVIOUS ESTIMATES OF UF_6 THERMAL DISSOCIATION RATE

In earlier work, Galkin and Tumanov (1971) used a variant of classical theory to predict the decomposition rate of UF_6, based on analogy to other inorganic polyhalides. The results of their computations, as presented in Fig. 3 of their text, yield the rate expression (in Arrhenius form):

$$k_{u1} = 4.6E9 \exp[-(70.2) \text{ kcal mol}^{-1}/RT] \text{ s}^{-1} \quad . \tag{6}$$

[In our notation, 4.6E9 represents 4.6×10^9 and is Galkin and Tumanov's estimate for the Arrhenius "pre-exponential" term [A-term, Eq.(2)] for k_{u1} in Eq. (1)]. In their classical model, Galkin and Tumanov assumed that only 3 "effective" oscillators (of the 15 total harmonic oscillators in UF_6) participate in the reaction (see Appendix), thus yielding a low value for the pre-exponential term (vide infra).

Schug and Wagner (1977) have used the conventional, single-pulse shock-tube technique to experimentally determine the thermal decomposition rate for UF_6 diluted in argon (total gas density 3E-6 to 4E-5 mol/cm^3, temperature range 1100 to 1450 K). Using this technique, relatively high temperatures can be obtained rapidly (from collisional translation-vibration (T-V) energy transfer from the argon propellent to the polyatomic reactant) and can be maintained for a convenient observation time (on the order of microseconds to milliseconds). Because of the shortness of the temperature pulse, little heat is transferred to the reactor walls, and homogeneous gas phase reactions may be studied. Some of the advantages and limitations of this technique are discussed by Belford and Strehlow (1969).

In the Schug and Wagner experiment, the real-time decrease in initial UF_6 concentration during the shock was monitored by ultraviolet (UV) light absorption. Radiation was supplied by a 200-W xenon-mercury lamp, with filtering at the detector side of the reactor to wavelengths between 220 and 370 nm. Light with wavelengths <415 nm is energetic enough to photolytically decompose UF_6 to yield fragments identical to those produced by thermal decomposition [Lewis et al. (1979); Lyman et al. (1985)]:

$$UF_6 + h\nu \rightarrow \beta\text{-}UF_5\ (s) + F \quad , \tag{7}$$

where β-UF_5 (s) is the condensation product of UF_5 [Lyman et al.(1985)]

It is unknown whether the monitoring technique used in the Schug and Wagner experiment significantly contributed to the magnitude of the observed reaction rate. Only the initial portion of absorption-time data were used in the calculation of reaction rates; at times greater than ~100 µs, the absorption-vs-time signal became distinctly nonlinear, presumably due to UF_5 + F recombination or to light absorption by UF_5 or its condensation products.

The pressure dependency of the measured rates suggested that the data were obtained in the transition between the low and high pressure-limiting domains. Schug and Wagner used a variant of the Kassel theory to extrapolate the data to estimate the first-order rate constant at the theoretical high-pressure limit (k_∞):

$$k_\infty = 3.3\text{E}16 \exp[-(70.3 \pm 4) \text{ kcal mol}^{-1}/RT] \text{ s}^{-1} . \tag{8}$$

Note that the pre-exponential term in Eq. (8) is several orders of magnitude greater than the theoretical estimate in Eq. (6) [Schug and Wagner have assumed 12.4 "effective" harmonic oscillators at 1300 K (see Appendix)]. Oref and Rabinovitch (1968) have criticized the use of "theoretical" methods such as the Kassel function to extrapolate rate data from the "fall-off" domain to the high-pressure limit, due to the difficulty in establishing an appropriate value for the number of "effective" oscillators to approximate the experimental curvature; however, we have applied an empirical procedure (such as Oref and Rabinovitch propose) to the Schug and Wagner data and have obtained a similar estimate for the high-pressure limit (see Appendix):

$$k_\infty = 1.1\text{E}16 \exp[-(67.8 \pm 2)\text{kcal mol}^{-1}/RT] \text{ s}^{-1} . \tag{9}$$

In addition, Lyman and Holland (1985) have applied the Rice-Ramsperger-Kassel-Marcus (RRKM) quantum theory to the data reported by Schug and Wagner; the high-pressure limit derived from this treatment was predicted to be:

$$k_\infty = 2.6\text{E}16 \exp[-69.7 \text{ kcal mol}^{-1}/RT] \text{ s}^{-1} . \tag{10}$$

Although there is good agreement for the extrapolated high-pressure limit using Schug and Wagner's data [see Eqs. (8-10)], we concluded that there was sufficient uncertainty in the actual data to warrant an independent investigation using different techniques for homogeneous pyrolysis and for product detection. These techniques are described in detail in the following sections.

LASER-POWERED HOMOGENEOUS PYROLYSIS

Laser-powered homogeneous pyrolysis (LPHP) is a relatively new technique in which a megawatt infrared (IR) laser is used to generate high bath temperatures for gas-phase reactions under strictly homogeneous conditions [Shaub and Bauer (1975)]. The bath gas mixture contains a sensitizer gas that absorbs the infrared laser radiation strongly and then collisionally transfers a significant portion of the energy to the desired reactant molecule without itself decomposing or chemically participating in the reaction process [Danen and Jang (1981)]. In typical experiments (see Table 1), total gas densities are on the order of 5 to 100 torr at ambient temperature (i.e, 2.7E-7 to 5.4E-6 mol/cm^3). At these densities, with use of a pulsed laser for multiphoton excitation, effective thermalization occurs within a few tens of nanoseconds, and heating continues for ~5 to 15 μs until the gas mixture is cooled by isentropic expansion behind a compression wave which moves radially outward at near-sonic velocity [McMillen et al. (1982)]. The short reaction time, together with diffusional mixing between laser pulses, minimizes side reactions. As in the shock tube technique, the reactor walls remain near ambient temperature, minimizing surface-catalyzed effects.

For quantitative work, the thermal profile must be known as a function of position and time throughout the reaction cell. These profiles can be estimated using gas dynamic models, but a simplified (and more accurate) procedure is to use an internal standard reactant (or "thermometer gas") with known kinetics similar to those of the compound under study [Dai et al. (1982), McMillen et al. (1982)]. Using a "relative-rate" approach [analogous to the comparative rate, single-pulse, shock-tube technique--see Belford and Strehlow (1969)], only an approximate estimate of the temporal and spatial variation of the temperature (as may be provided by a gas dynamic model) is required for accurate rate constant measurements [Dai et al. (1982)].

McMillen and co-workers (1982) derived a simplified data treatment which eliminates the need for explicit knowledge of the temperature corresponding to a particular measurement of a rate constant, ku. In their formulation [see also Dai et al. (1982)],

$$\log F_u = \log A_u + (1 - E_u/E_s)\log t - (E_u/E_s)\log A_s + (E_u/E_s) \log F_s \ , \tag{11}$$

where A and E are Arrhenius terms [see Eq. (2)], subscripts u and s refer to the molecules with "unknown" and "standard" (i.e., known) kinetic properties, t is effective reaction time (s), and F = kt ~ ΔP/Po is the fractional decomposition per laser shot.

Both SF_6 and SiF_4 have frequently been used as sensitizers for multiphoton excitation by CO_2 lasers (see Table 1). However, SF_6 itself has been found to decompose under conditions of modest fluence from a pulsed CO_2 laser [Danen and Jang (1981), Olszyna et al. (1977)]. In addition to its self-decomposition (primarily to SF_4), excited SF_6 can rapidly transfer near-resonant vibrational energy to UF_6 (the reactant of interest in our investigation); the R-branch of the υ_4 band of SF_6 overlaps the υ_3 band of UF_6 [Karve et al. (1981)]. Karve et al. report rapid vibrational energy exchange between SF_6 and UF_6 (within a few tens of nanoseconds) after absorption of laser radiation by SF_6 and specifically rule out a significant pyrolytic contribution in the multiphoton

Table 1. Laser-powered sensitized thermal reactions

Reference	CO_2 laser system	Sensitizer	Substrate	"Thermometer" gas	"Bath" gas[a]	Total gas density (mol/cm^3)	Nominal reaction time (μs)	Effective temperature range (K)
Schaub and Bauer (1975)	CW_v chopped at 1 Hz (λ = 10.67 μm)	SF_6	Various organic compounds	Cyclopropane, etc.	Ar	(5.4-8.1)E-6	$\geq$500	~700-1000
Farneth et al. (1976)	Pulsed (λ = 9.55 μm)	CH_3F	Tetra methyl-1,2-dioxetane	(Chemiluminescence)	CH_3F	(0.1-1.6)E-6	--	~400-500
Steel et al. (1979)	Pulsed (λ = 9.29 μm)	NH_3	Cyclobutanone	(Cyclobutanone)	NH_3	2.7E-6	~10-20	~1020-1320
Lewis et al. (1980)	Pulsed (λ = 10.57 μm)	SF_6	Aromatic nitro comppounds	--	SF_6 + Ar	(1.7-2.3)E-6	[~20][b]	~1000-1200
Smith and Laine (1981)	Pulsed (λ = 10.59 μm)	SF_6	$Fe(CO)_5$	CH_4 (IR emission)	SO_2	5.4E-6	~10	~1000
Comita et al. (1981)	Pulsed (λ = 9.73 μm)	SiF_4	Tetralin	--	SiF_4	(2.7-5.4)E-6	--	~900-1900 (Tmax)
Tsang et al. (1982)	Pulsed (λ = 9.74 μm)	SiF_4	1,2-dichloropropane	--	SiF_4	8.6E-7	>1	~1100
McMillen et al. (1982)	Pulsed (λ = 10.59 μm)	SF_6	AZO compounds	t-butyl acetate, etc.	CO_2	5.4E-6	~5-15	~780-1060
Dai et al. (1982)	Pulsed (λ = 9.73 μm)	SiF_4	Chloroalkanes	Ethyl chloride	SiF_4	2.8E-7	~10-30	~1150-1350
Jasinski and Estes (1985)	Pulsed (λ = 9.76 μm)	SiF_4	Silane	Cholopropane	SiF_4	1.1E-6	[~10][b]	~750-1000
This work	Pulsed (λ = 9.73 μm)	SiF_4	UF_6	Ethyl chloride (external standard)	CF_3Cl + SiF_4	(1.6-8.1)E-6	[~20][b]	~1050-1350

[a] Major constituent in mixture.
[b] Assumed value.

excitation (at 947 cm^{-1}) of a mixture of SF_6 and UF_6. Angelie and coworkers (1982) have also examined SF_6-sensitized dissociation of UF_6, with and without H_2 as a scavenger for atomic fluorine reaction product. When SF_6 itself was irradiated with a CO_2 laser, the main decomposition product was SF_4 (i.e., self-decomposition). When UF_6 was added to the SF_6, dissociation of SF_6 was drastically quenched. They propose several potential reaction mechanisms to account for this observation--the first is efficient deactivation of SF_6 by (near-resonant) V-V energy transfer to UF_6:

$$SF_6 + h\upsilon \rightarrow SF_6^* \ , \tag{12}$$

$$SF_6^* + UF_6 \rightarrow SF_6 + UF_6^* \ , \tag{13}$$

$$UF_6^* \rightarrow UF_5 + F \ . \tag{14}$$

$$F + F + M \xrightarrow{k_{15}} F_2 + M \ . \tag{15}$$

[In Eq. (15), "M" designates a "third-body" collision partner for energy transfer.] An alternative mechanism is SF_6 dissociation, followed by an efficient reaction with UF_6 to regenerate SF_6:

$$SF_6 + h\upsilon \rightarrow SF_5 + F \ . \tag{16}$$

$$SF_5 + UF_6 \rightarrow SF_6 + UF_5 \ . \tag{17}$$

Either mechanism would account for the preferential reduction of UF_6 in the presence of SF_6.

We concluded that use of SF_6 as a sensitizer for LPHP of UF_6 would be unsatisfactory due to the possibility of nonpyrolitic mechanisms, including near-resonant V-V energy transfer and decomposition of SF_6, to produce species which may be directly reactive with UF_6 [see Eq. (16)]. Silicon tetrafluoride (SiF_4) is stable at considerably higher laser fluence values due to its high bond dissociation energy (see Table 2). Olszyna et al. (1977) have discussed the advantages of SiF_4 as an inert sensitizer, and we have used it for this purpose in the current investigation.

Table 2. Bond dissociation energies (D°_{298}) for selected compounds

Compound	Bond	Bond dissociation energy (kcal/mol at 298 K)	Reference
SiF_4	$F\text{-}SiF_3$	160	Walsh (1981)
		142	Danen and Jang (1981)
UF_4	$F\text{-}UF_3$	148.2	Lau and Hildenbrand (1977)
HF	F-H	136.2	CRC, 66th ed. (1985)
CF_4	$F\text{-}CF_3$	130	Walsh (1981)
CF_3Cl	$F\text{-}CF_2Cl$	117	CRC, 66th ed. (1985)
	$Cl\text{-}CF_3$	86	
HCl	H-Cl	103.1	CRC, 66th ed. (1985)
UF_5	$F\text{-}UF_4$	102	CRC, 66th ed. (1985)
SF_6	$F\text{-}SF_5$	92	Lyman (1977)
C_2H_5Cl	$Cl\text{-}C_2H_5$	80.4	Howlett (1952)
UF_6	$F\text{-}UF_5$	69.2 ± 4.6	Compton (1977)
		68.3 ± 3.5	Hildenbrand (1977)
		67.7 ± 5.6	Schug and Wagner (1977)
FCl	F-Cl	61.2	CRC, 66th ed. (1985)
Cl_2	Cl-Cl	58.1	CRC, 66th ed. (1985)
F_2	F-F	37.8	CRC, 66th ed. (1985)

EXPERIMENTAL

GAS-HANDLING SYSTEM

The experimental arrangement is schematically depicted in Fig. 1. Prior to each experiment, the gas-handling system is evacuated, then refilled from the gas manifold. The constituent with the lowest partial pressure in the final mixture is added first, with subsequent addition of reagent gases in the order of increasing partial pressure. Each gas addition is monitored by pressure change and the final total system

DWG. NO. K/G-86-1458 (U)

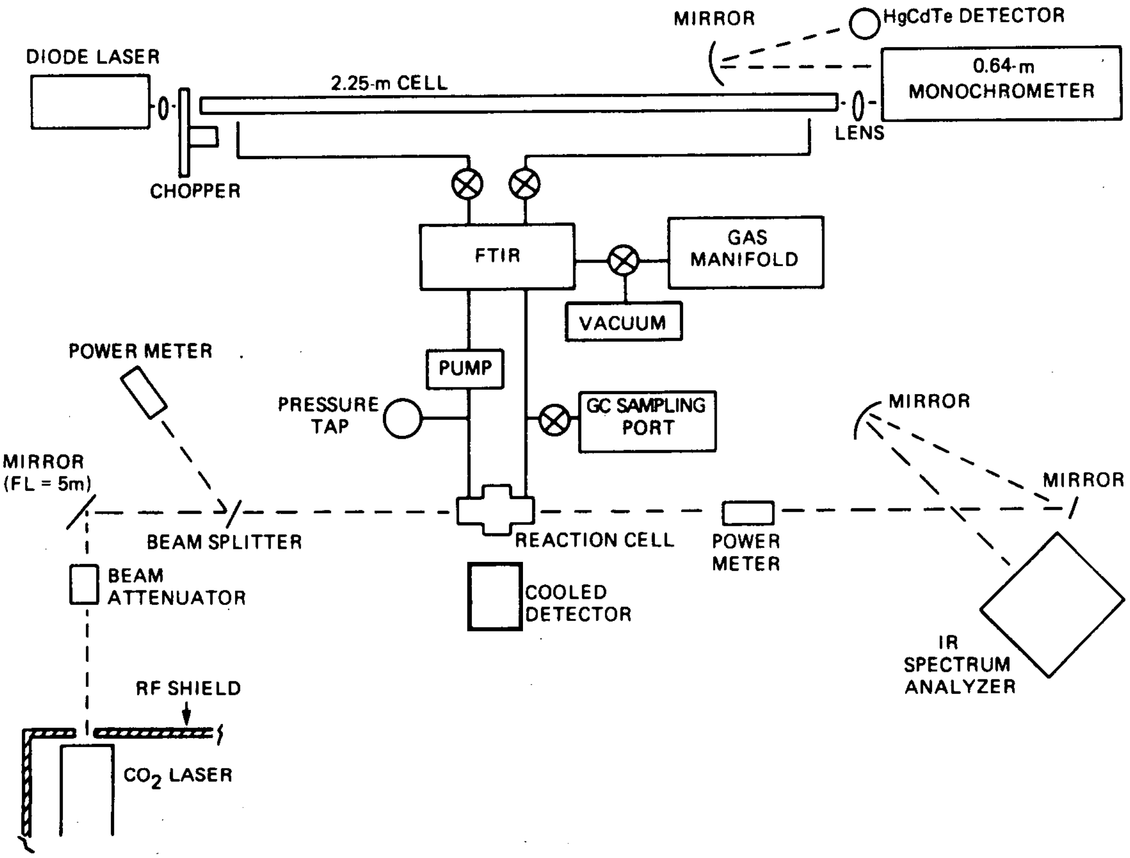

Fig. 1. Schematic for LPHP experiment.

pressure. Between each addition, the system is valved off and the manifold and fill lines evacuated. Then the manifold pressure of the next constituent to be added is raised to a pressure value slightly above that of the previous mixture. The valve to the gas circulation system is opened, and the total system pressure is adjusted to the target value by addition of the appropriate constituent. Gas mixture compositions for the major experiments described in the text are given in Table 3.

Table 3. Gas mixtures for laser-powered homogeneous pyrolysis

	P = partial pressure (torr) at 25°C (298 K) [M] = density (mole/cm^3)			
Data set	SiF_4	Reactant gas	CF_3Cl	Total
A	P = 15 [M] = 8.1E-7	P = 5 [M] = 2.7E-7	P = 10 [M] = 5.4E-7	P = 30 [M] = 1.6E-6
B	P = 15 [M] = 8.1E-7	P = 10 [M] = 5.4E-7	P = 50 [M] = 2.7E-7	P = 75 [M] = 4.0E-6
C	P = 15 [M] = 8.1E-7	P = 10 [M] = 5.4E-7	P = 100 [M] = 5.4E-7	P = 125 [M] = 6.7E-6

Gases within the system are mixed and recirculated using a Metal Bellows Corporation, Model MB-41, pump; components of the pump contacting the gas stream are made from series 300 stainless steel or Teflon. Performance of this pump assembly in our system was measured with a Hastings All-1KP flow meter using nitrogen gas (see Fig. 2). Gas transfer lines were assembled from 1/4-in. (0.64-cm) ID nickel tubing with nickel-plated copper fittings.

The entire gas-handling system, including optical cells, was preconditioned by the batch-wise exposure to ClF_3 at room temperature. Passivation of surfaces was considered satisfactory when UF_6 (partial pressure ~10 torr in N_2 diluent) demonstrated long-term stability (i.e., for several hours) when recirculated through the system.

CELL CONSTRUCTION

For some preliminary experiments, a relatively long (~42-cm) reaction cell was constructed from series 304 stainless steel Varian Conflats® (see Fig. 3A). A KBr lens (focal length = 47 cm) was placed before the front window, producing a softly focused beam (~1 mm) at the center of the cell. An emission window, either synthetic sapphire (for visible and near IR) or AgCl (for extended-range IR), was located at the center of the cell, orthogonal to the laser beam path. A cooled detector

DWG. NO. K/G-87-366 (U)

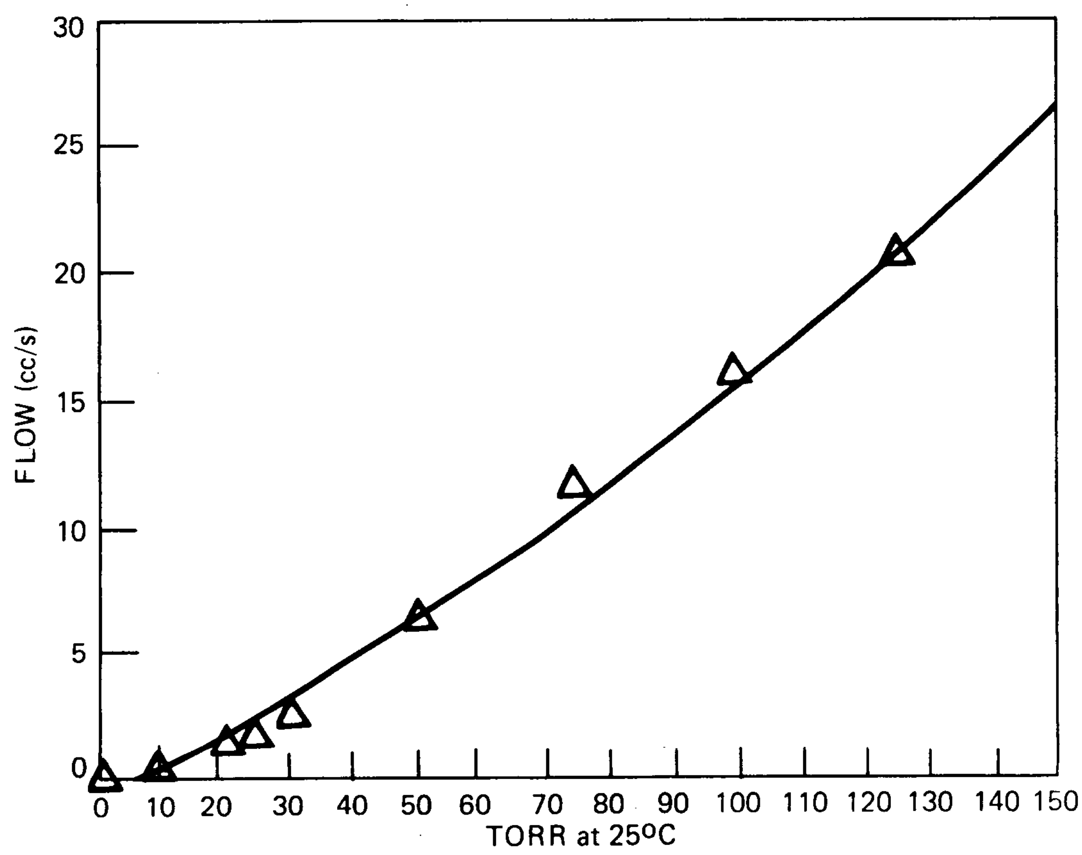

Fig. 2. Nitrogen mass flow rate with the use of MB-41 pump.

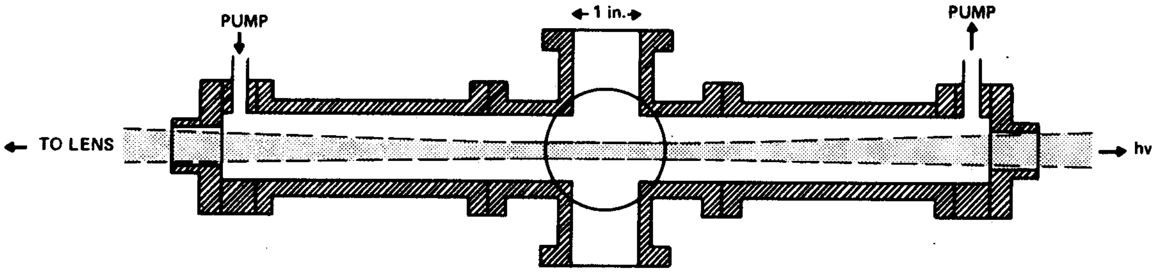

A) CELL GEOMETRY USED IN INITIAL STUDIES

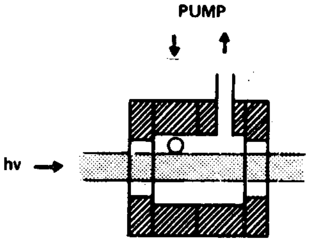

B) CELL GEOMETRY USED IN FINAL STUDIES

Fig. 3. Reactor cell construction.

(photomultiplier tube or copper-doped germanium detector) was mounted at the emission window. For this configuration, beam volume within the cylindrical reaction cell, as estimated from burn patterns, was ~11 cm^3, and total volume (exclusive of manifold, but including the long-path IR monitoring cell) was 1229.6 cm^3.

Initially, cell windows were KBr with a CaF_2 evaporative coating on the inner surface. These windows demonstrated adequate resistance against chemical attack by corrosive gaseous fluorides [see also Swope (1971)], but they were readily damaged by high fluence IR laser radiation. Zinc selenide windows, antireflectance (AR) coated on both sides to withstand 50 GW/cm^2, were subsequently used; the AR coating on the inner surface was evaporated PbF_2 (Type IV, II-VI Corp.). These windows demonstrated excellent stability to high-fluence IR radiation and to corrosive gases, although the windows did tend to form a film on the inner surface with a long-duration exposure to UF_6 pyrolysis products. Each window transmitted ~61% of the laser beam at the 9.73-μm wavelength.

The long-path (2.25-m) IR-monitoring cell depicted in Fig. 1 was used in conjunction with a Laser Analytics diode laser spectrometer to increase detection sensitivity. A diode operating in the vicinity of 760 cm^{-1} in the P branch of ClF allowed detection of that species at partial pressures of ~0.005 to 0.10 torr. A diode operating near 1280 cm^{-1} was used to monitor CF_4 in some preliminary studies.

For the majority of experiments described in the text, we used a shorter cylindrical reaction cell, 1.5 in. (3.8 cm) ID × 2 in. (5.3 cm) long (active volume ~58 cm^3) as shown in Fig. 3B. For the partial pressures of SiF_4 used in these experiments, the path length was optically thin, and (without the use of the KBr lens) energy deposition was essentially uniform; this helps prevent nonuniform axial temperatures and longitudinal acoustic waves. In this configuration, beam volume within the cell was ~8.2 cm^3, and total volume (exclusive of manifold and long-path IR cell) was 169.8 cm^3.

STANDARDS, CALIBRATION, AND DETECTION OF REAGENT GASES

Normal assay UF_6 was obtained from a large inventory manufactured by National Lead of Ohio and was purified by flashing off noncondensables and high-vapor pressure fractions. The remaining UF_6 was then fractionally sublimed to separate UF_6 from less volatile components.

Liquid chloroethane (C_2H_5Cl) was purchased from Eastman Kodak Company (Catalog No. 1075). Lecture bottles of Freon 13 (CF_3Cl), Freon 14 (CF_4), silicon tetrafluoride, and ethylene (stated purities ≥99%) were purchased from Matheson Gas Products.

The CF_3Cl reagent gas, as received, appeared to contain ~1% CF_4 as an impurity, as determined from IR spectroscopy. A sample of this reagent was transferred to a smaller cylinder equilibrated in a n-propanol, liquid N_2 slush bath at -123°C [see Rabek (1982)], and the more volatile CF_4 component was preferentially removed by fractional distillation. The residual CF_4 component in the purified CF_3Cl was ~0.13% (mole basis).

The concentration of various gases was measured in a 6-cm path IR flow cell with silver chloride windows, mounted in a Nicolet Analytical Instruments, Model MX-1, Fourier transform infrared (FTIR) spectrophotometer, at nominal resolutions of 1 or 2 cm^{-1}. Partial pressures of UF_6 were monitored at 626 or 631 cm^{-1}; CF_4 at 1281 or 1283 cm^{-1}; C_2H_5Cl at 677, 686, or 1298 cm^{-1}; C_2H_4 at 949 cm^{-1}; and C_2H_2 at 730 cm^{-1}. Because total pressures were low (≤150 torr at 25°C), pressure-broadening effects in complex gas mixtures were estimated by dilution of the constituent of interest in CF_3Cl solution (major constituent of the reaction mixture in the LPHP experiment, see Table 1); a typical calibration curve is illustrated in Fig. 4. The calibration for organic constituents was also checked by withdrawing a sample of gas mixture for independent analysis by gas chromatography (GC) as seen in Fig. 1; GC of gas mixtures containing corrosive UF_6 was not attempted.

CO_2 LASER SYSTEM

A Lumonics Model TEA-103-2 grating-tuned CO_2 laser, operating on the 9 P(40) line (1027.4 cm^{-1}) was used to excite the strong υ_3 band of SiF_4 (1029.6 cm^{-1}). Laser frequency was verified using an Optical Engineering, Inc., Model 16-A, CO_2 laser spectrum analyzer. Each laser pulse consisted of an initial sharp feature of ~70-ns duration, followed by a long, but much less intense, tail. Typical laser output at this transition was ~1.5 J, with a pulse-to-pulse variation of ±10% at a repetition rate of ~0.15 s^{-1}. A slow repetition rate allows complete mixing by diffusion and convection (see Fig. 2) between two consecutive laser shots; small fractional conversion, coupled with efficient mixing, helps to minimize the effect of any secondary reactions.

The output coupler of the laser was AR-coated germanium (51 mm in diam × 5 mm thick); side 1 (inner) had a radius of 25 m, with 84% reflectivity, and side 2 (outer) had a radius of 10.75 m. An intercavity aperture was used to reduce transverse modes from the laser, and an external aperture was used to select the nearly uniform energy central portion of the beam. The beam profile was approximately Gaussian.

The beam path is illustrated in Fig. 1. Beam energy was attenuated in steps by placing uncoated potassium bromide or germanium flats in the beam path, giving average pulse energies of 0.5 to 1.5 J. The beam reflects off a copper mirror with a radius of 0.5 m to give a soft focus in the center of the reaction cell; nominal beam area (estimated from burn patterns) is ~1.6 cm^2 (reactor cross-section is ~11.4 cm). Approximately 5% of the input beam is directed from a potassium bromide beam splitter into a Laser Precision Corp., Model RJP-736, large-area (20 cm^2) disk calorimeter, and the signal is monitored using a Laser Precision Corp., Model RJ7200, energy ratiometer. This served as the power meter for laser input energy to the pyrolysis cell. Energy transmitted

DWG. NO. K/G-86-1456 (U)

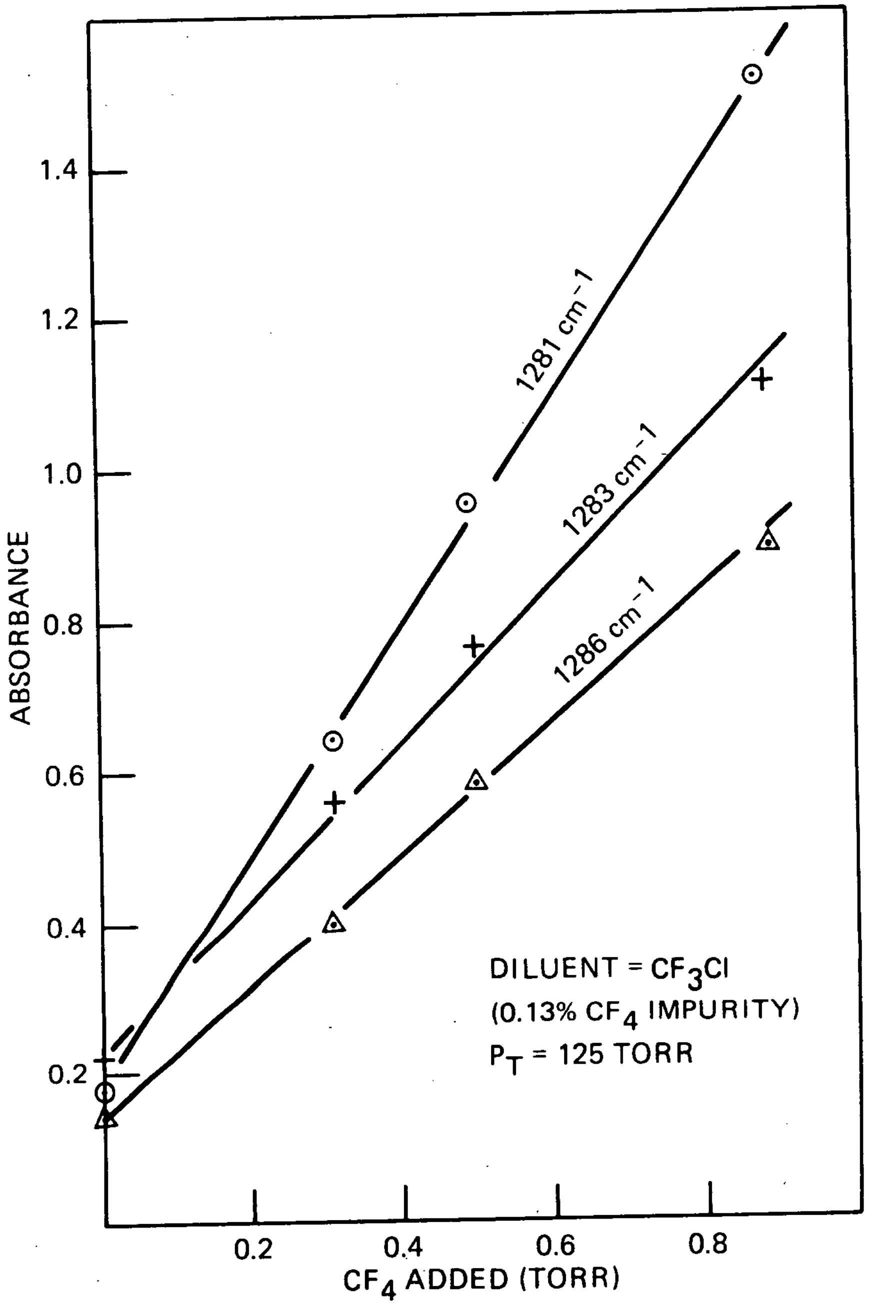

Fig. 4. Calibration for CF_4 concentration in CF_3Cl diluent, as measured by FTIR spectroscopy (6-cm optical pathlength).

through the reaction cell was monitored by a second Laser Precision power meter assembly. These power meter measurements were periodically calibrated against a previously calibrated Scientech, Model 38-0102, volume-absorbing calorimeter with isoperibol enclosure.

RESULTS AND DISCUSSION

SELECTION OF A SENSITIZER

As illustrated in Table 4, the SiF_4 partial pressure in the LPHP reaction mixture had a significant effect on the effective temperature produced within the pyrolysis cell, as judged by the yield of CF_4 indicator species for atomic fluorine decomposition product from UF6 (see section titled Selection of an Atomic Fluorine Trapping Agent). In Table 4, mixtures I-IV represent room-temperature SiF_4 partial pressures of 5, 10, 15, and 20 torr, respectively. Figure 5 illustrates the change in CF_4 concentration (as monitored by FTIR spectroscopy) during LPHP using gas mix III, Table 4 (i.e., at 15 torr SiF_4). At the lowest SiF_4 partial pressure tested, there was essentially no change in the CF_4 indicator upon laser irradiation; higher partial pressures produced significant indicator species. Apparently, at the laser fluence used in this study, there is a minimum threshold concentration of sensitizer necessary to produce detectable decomposition of UF_6. However, as shown by the data from mix V in Table 4, some production of CF_4 indicator can occur without UF_6 at high concentrations of sensitizer coupled to high

Table 4. Effect of SiF_4 concentration on apparent UF_6 thermal decomposition rate

	Gas composition (mol/cm³) × E6					Δ (CF_4/N)*
Mix	SiF_4	UF_6	CF_3Cl	N_2	Total	(mol/cm³) × 1E11
I	0.27	0.27	0.27	0.53	1.34	-0.02
II	0.53	0.27	0.27	0.27	1.34	0.19
III	0.80	0.27	0.27	0	1.34	1.25
IV	1.07	0.27	0.27	0	1.61	2.97
V	1.07	0	0.27	0	1.34	0.40

*Δ (CF_4/N) is the change in CF_4 concentration within the irradiation zone per laser pulse at an average incident fluence of 1.45 ± 0.04 J. (Reactor geometry as in Fig. 3A; ratio of irradiated zone to total volume = 1:18.7.)

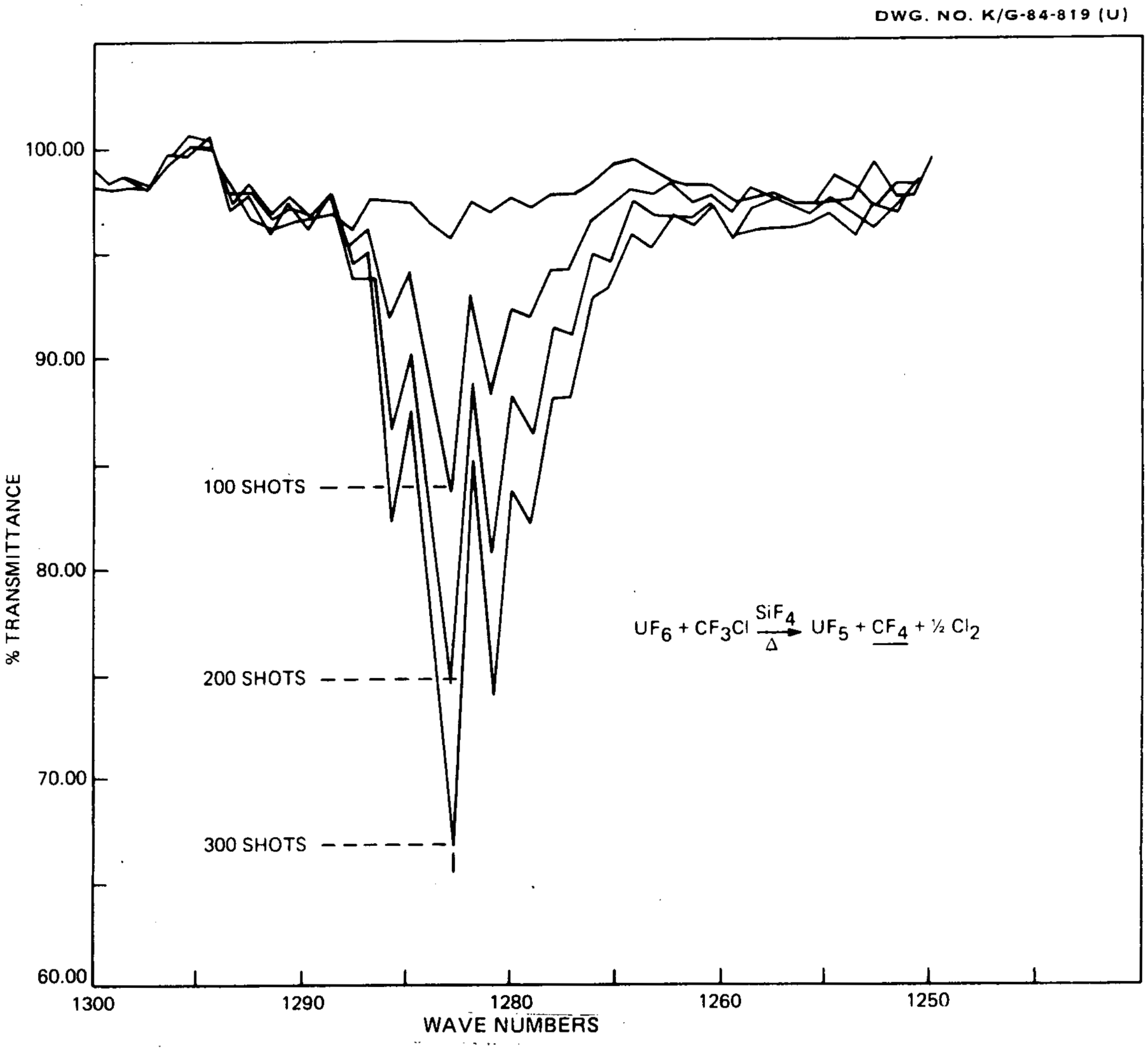

Fig. 5. Production of CF_4 indicator, as monitored by FTIR spectroscopy, during pulsed laser pyrolysis of UF_6 with SiF_4 sensitizer.

laser fluence; at a partial pressure of 20 torr SiF_4, this "blank" rate of indicator production is ~13% of the rate observed in the presence of UF_6 reactant. The origin of this "blank" reaction is not known but is probably related to the dissociation of the $Cl-CF_3$ bond (86 kcal/mol, see Table 2), to produce CF_3 radical, which then abstracts a fluorine atom to form CF_4. To minimize the production of indicator species from sources other than UF_6 decomposition, we have used a room-temperature partial pressure of 15 torr (8.0E-7 mol/cm^3) SiF_4 sensitizer in our LPHP experiments, and effective reaction temperature was varied by variation of laser fluence.

SELECTION OF A "THERMOMETER" GAS

The use of an internal standard, with well-accepted Arrhenius parameters, facilitates the estimation of corresponding parameters for the "unknown" reactant using Eq. (11) or similar treatment [McMillen et al. (1982), Dai et al. (1982)]. In particular, the use of a "thermometer gas" compensates for uncertainties in the temporal and spatial distribution of thermal energy in the reaction vessel. McMillen (1982) discusses the conditions under which data reduction using Eq. (11) is valid and most accurate.

The better the Arrhenius parameters of the "standard" and the "unknown" reactants are "matched," the less the relative yields depend on the exact temperature-time profile. For example, the energy of activation for the "unknown" is derived in Eq. (11) from the ratio E_u/E_s, so that the resulting estimate of the activation energy of the "unknown" compound is very "rugged" in the sense that rate ratios will be much closer to the high-pressure limiting values than are the absolute rates themselves [Dai et al. (1982)]. McMillen observes that for $0.9 < (E_u/E_s) < 1.1$, even a tenfold error in the estimated reaction time, t, will result in an error in the derived estimate of log Au of only 0.1 log units; such error is smaller than, or comparable in magnitude to, the typical uncertainty in parameter estimates from "average" experimental measurements of absolute rates. Benson and O'Neal (1970) estimate the probable error in the Arrhenius A-factor due to the uncertainty in activation energy:

$$\Delta(\log A) = \Delta(Ea)/2.3RT \ , \qquad (18)$$

where $\Delta(Ea)$ is the uncertainty in the activation energy (typically on the order of 5%). (e.g., a 4-kcal uncertainty in an activation energy of 70 kcal, measured at a mean temperature of 1300 K [see Eq. (8)] would be associated with an uncertainty in log A of ±0.7 log units).

In our data reduction using Eq. (11), we have assumed a median effective reaction time, t, of 20 μs, comparable in magnitude to the reaction times estimated or assumed by other investigators using the LPHP technique in reactors of similar geometry and with similar gas densities (see Table 1). In our experiment, we attempted a direct estimate of the time evolution of the temperature in the heated region by measuring the laser-induced IR thermal fluorescence emission of gas constituents triggered by the laser pulse; a similar technique was used to derive estimates of effective reaction times in the experiments reported by Smith and Laine (1981), McMillen et al. (1982), and Dai et al. (1982). However, RF noise pickup from our laser or microphonics in our detector (mounted orthogonally to laser beam propagation, see Fig.1) precluded accurate measurement of fluorescence emission during the first 30 µs subsequent to the laser pulse. Qualitatively, the remainder of the recorded signal for gas mixture A (see Table 3) strongly resembled the data reported by Dai et al. (1982), with apparent cooling (due to gas expansion) between ~ 30 to 100 µs, followed by a slight reheating (attributed to the reflected shockwave) peaking at about 160 µs.

Due to the aggressive reaction between UF_6 and hydrocarbons, especially at elevated temperature, it was necessary to use the thermometer gas in a separate LPHP experiment (i.e., as an "external standard"), replacing UF_6 as the reagent gas, under otherwise identical conditions of laser fluence and composition of other gases (see Table 2).

Cyclopropane ($c\text{-}C_3H_6$) and ethyl chloride (C_2H_5Cl) are good candidates for a thermometer gas; some reported estimates for their high-pressure Arrhenius parameters are given in Table 5 (note that there is a considerable range of estimated Arrhenius parameters, even for well-studied unimolecular reactions). As seen in the table, the Arrhenius parameters for cyclopropane are somewhat more similar to those reported by Schug and Wagner for UF_6 than are the parameters for ethyl chloride, i.e., E_u/E_s ratios of ~1.1 for cyclopropane standard vs 1.2 for C_2H_5Cl standard. However, use of SiF_4 sensitizer (as described previously) with CO_2-laser excitation at a 9.73-µm wavelength could result in direct photolytic dissociation of cyclopropane, because the spectrum of cyclopropane (as well as propene product) overlaps that of SiF_4 in this spectral region. In addition, high temperature shock-tube data for cyclopropane isomerization are reported to demonstrate "anomalous" kinetics [see Barnard et al. (1974)].

We elected to use ethyl chloride for our "thermometer gas," using the high-pressure Arrhenius parameters defined by Holbrook and Marsh (1967) (see Table 5). Ethyl chloride has little or no absorbance at 9.73 µm; ethylene product has only weak absorbance at this wavelength (even when pressure-broadened at high gas density); and acetylene, the unimolecular decomposition product of ethylene, is transparent at this wavelength. For quantitation of ethyl chloride decomposition, we monitored ethylene and acetylene concentrations (see Experimental section). Figure 6 illustrates the increase in ethylene (C_2H_4) product during an LPHP experiment in a mixture of C_2H_5Cl, CF_3Cl, and SiF_4, as monitored by FTIR spectroscopy (at 2-cm^{-1} resolution). At high laser fluence, LPHP of C_2H_5Cl also produced a new absorption at 730 cm^{-1}, characteristic of acetylene (C_2H_2); this was assumed to be due to subsequent thermal

Table 5. High pressure-limiting Arrhenius parameters for selected unimolecular reactions

Reaction	Log A	Ea (kcal/mol)	Log k_∞[a] (T = 1000 K)	Reference
$UF_6 \rightarrow UF_5 + F$	16.52	70.3 (±4)	+1.16	Schug and Wagner (1977)
Cylopropane → Propene	15.16	65.4	+0.87	Benson and O'Neal (1970)[b]
	15.17	65.0	+0.96	Pritchard et al. (1953); Chambers and Kistiakowsky (1934)
	15.27	65.6	+0.94	Yau and Pritchard (1978)
	15.45	65.6	+1.11	Dillard and Heydtmann (1977)
	15.52	65.5	+1.21	Furue and Pacey (1982)
Ethyl chloride → Ethylene + HCl	13.2	56.5	+0.85	Benson and O'Neal (1970)[b]
	14.03 (±0.4)	58.43 (±1.5)	+1.26	Holbrook and Marsh (1967)
	13.8	57.4	+1.26	Dai et al. (1982)[b]
	13.33 (±0.1)	56.3 (±0.3)	+1.03	Heydtmann et al. (1975)
	14.6	60.8	+1.31	Howlett (1952)
	13.84	57.8	+1.21	Evans et al. (1978)

[a] $\text{Log } k_\infty = \text{Log } A - Ea/2.3RT$.

[b] Values assumed for calculations in cited text.

DWG. NO. K/G-84-817 (U)

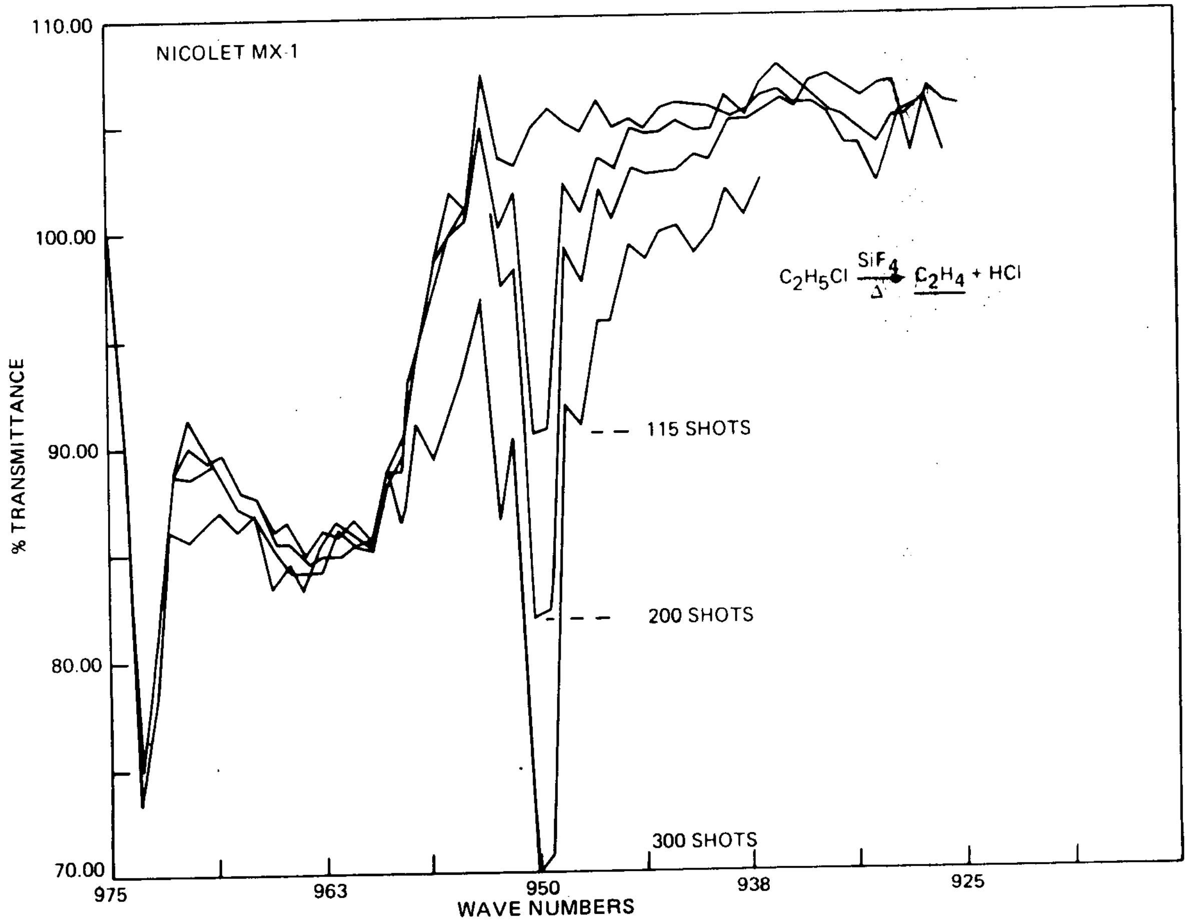

Fig. 6. Production of ethylene (C_2H_4), as monitored by FTIR spectroscopy, during pulsed laser pyrolysis of ethyl chloride (C_2H_5Cl) with SiF_4 sensitizer.

dissociation of C_2H_4. LPHP with C_2H_4 as the reactant gas (conditions as in Table 3, data set A), vs C_2H_5Cl as an "external standard," yielded the Arrhenius parameters for C_2H_4 given in Table 6, in which our results are compared with those reported previously using shock tube techniques and conventional static thermal reactors. As in the shock tube experiments, the LPHP decomposition product was C_2H_2, with no indication (by IR spectroscopy) of other hydrocarbons formed from surface-catalyzed chain reactions (cf static reactors). The activation energies determined by the LPHP and shock tube experiments are in good agreement; the Arrhenius pre-exponential factor determined from the LPHP experiment may be somewhat high, perhaps reflecting a minor photolytic contribution to the overall dissociation.

Table 6. Thermal decomposition of ethylene (C_2H_4)

Technique	Conditions	Predominant mechanism[a]	Log A	Ea (kcal/mol)	Reference
Shock tube	C_2H_4 in Ar T = 1250 - 1800 K P = 1700 - 4300 torr	Uni	8.41	40	Kozlov and Knorre (1963)
	T = 1300 - 1800 K 1170 - 1425 K	Uni	8.87 11.95	46.5 65	Skinner and Sokolski (1960)
	T = 1400 - 300 K	Uni	?	73	Asaba et al. (1962)
LPHP	C_2H_4 in SiF_4 + CF_3Cl (M = 8E - 7 mol/cm^3) T = 1140 - 1290 K	Uni	14.73 (±0.1)	66.2 (±0.6)	This work
Static	Self-medium T near 725 K	Chain	14.7	70.8	Delliste et al. (1981)
	T = 770 - 870 K P = 50 - 300 torr	Chain	14.82	64	Boyd et al. (1968)
	T near 825 K	Chain	?	60 ± 6	Nazarov and Torban (1966)

[a] Uni = Unimolecular ($C_2H_4 \rightarrow C_2H_2 + H_2$). Chain = radical reaction ($C_2H_2 \rightarrow C_2H_6 + C_4H_8$, etc.).

SELECTION OF AN ATOMIC FLUORINE TRAPPING AGENT

The recombination reaction between UF_5 and atomic fluorine [reverse reaction Eq. (3)] is relatively rapid [Lyman et al. (1985)]. (Note that UF_5 which does not recombine with atomic fluorine tends to polymerize and to condense out as solid β-UF_5 near room temperature [Lewis (1979), Lyman (1985)].

If one is to determine the unimolecular decomposition of UF_6, one must either follow the real-time change in UF_6 composition during the first few milliseconds of the reaction (as in the Schug and Wagner experiment), or (because it is difficult to make selective, real-time measurements of the transient, highly reactive UF_5 or F products), one must trap the atomic fluorine product by a rapid indicator reaction to yield a stable, easily monitored species.

Reaction kinetics for many reactions of atomic fluorine have been reviewed [see Zetzsch (1976), Jones and Skolnik (1976), Foon and Kaufman (1975), Baulch et al. (1981)]. Estimated rate constants for some reactions of interest, including selected reactions of atomic fluorine, are given in Table 7. Molecular hydrogen reacts very rapidly with atomic fluorine (see Table 7), and it has been used as a trapping agent for atomic fluorine produced by the UV-photolysis of UF_6 [see Lewis et al. (1979), Andreoni et al. (1980), Lyman et al. (1985)]:

$$H_2 + F \xrightarrow{k_{19}} HF + H \ (\Delta H_{298} = -31.6 \text{ kcal/mol}) \ . \qquad (19)$$

The primary quantum yield (ϕ) for a photolytic reaction of the type:

$$A + h\upsilon \rightarrow B \qquad (20)$$

is defined (see Rabek, 1982) as

$$\phi = \frac{\text{number of molecules, radicals, or ions of B formed}}{\text{number of quanta absorbed by A}} \ . \qquad (21)$$

In the absence of trapping agent, the apparent quantum yield for the photolysis of UF_6 at moderate gas densities is less than unity, due to UF_5 + F recombination; however in the presence of H_2, the apparent quantum yield is substantially above unity [Andreoni et al. (1980), Lewis et al. (1979)]. This indicates a net reduction of UF_6 by H_2 or fluorine abstraction from UF_6 by atomic hydrogen. The mechanism and kinetics of the gas phase reactions between UF_6 and H_2 are complicated, with solid UF_4 being formed at elevated temperatures [Tumanov and Galkin (1971), Myerson and Chuldzinski (1981), Barber (1985)]. Barber (1985) suggests that the initial step in the reduction of UF_6 by H_2 is the following:

$$UF_6 + H_2 \xrightarrow{k_{22}} UF_5 + HF + H \ (\Delta H_{298} = +37.6 \text{ kcal/mol}) \ . \qquad (22)$$

The endothermic nature of reaction Eq. (22) suggests that F abstraction by atomic hydrogen is important in UF_6 reduction by hydrogen [Barber (1985)]:

Table 7. Estimated rate constants for selected reactions

Text		Log k = log A - Ea/2.3 RT			
eqn.	Reaction	Log_{10} A	Ea (kcal/mol)	k (T)	Reference
(1)	$UF_6 \rightarrow UF_5 + F$	16.52	70.3	k (1200 K) = 5.2E-3 (s^{-1})	Schug and Wagner (1977)
(1)	$UF_5 + F \rightarrow UF_6$	~12.6	~0.72	k (300 K) = 1.2E-12 k (1200 K) = 3E-12 (cm^3/mol-s)	Lyman et al. (1985) and personal communication
(15)	$F + F + M \rightarrow F_2 + M$ (M = Ar)	8.51	3.19	k (1200 K) = 4E-9 ($cm^6\ mol^{-2}\ s^{-1}$)	Baulch et al. (1981)
(19)	$H_2 + F \rightarrow HF + H$	13.4	0.9	k (300 K) = 1.5E-13 (cm^3/mol-s)	Jones and Skolnik (1976)
(22)	$UF_6 + H_2 \rightarrow UF_5 + HF + H$	15.9	34.5	k (300 K) = 5.9E-10 k (800 K) = 2.9E-6 (cm^3/mol-s)	Barber (1985)
(23)	$UF_6 + H \rightarrow UF_5 + HF$	14	4.2	k (300 K) = 8.7E-10 (cm^3/mol-s)	Rienacker (1981)
(25)	$Cl_2 + F \rightarrow ClF + Cl$	14.74	1.4	k (300 K) = 5.2E-13 (cm^3/mol-s)	Warnatz et al. (1971)
(28)	$Cl_2 + M \rightarrow Cl + Cl + M$ (M = Ar)	13.36	23.6	k (1200 K) = 6.5E-4 (cm^3/mol-s)	Baulch et al. (1981)
(30)	$CF_3Cl + F \rightarrow ClF + CF_3$	13.8	20.9	k (300 K) = 0.04 k (1200 K) = 9.7E+6	Foon and Tait (1972)
				k (300 K) ≤ 1E+9 (cm^3/mol-s)	Zetzsch (1971)

$$UF_6 + H \rightarrow UF_5 + HF \ (\Delta H_{298} = -66.6 \text{ kcal/mol}) \ , \qquad (23)$$

$$UF_5 + H \rightarrow UF_4 + HF \ (\Delta H_{298} = -36.0 \text{ kcal/mol}) \ . \qquad (24)$$

Because of the anticipated complications with use of hydrogen with UF_6, we sought alternative F-atom reagents. In some initial studies, we investigated the use of chlorine, which is known to react rapidly and quantitatively with atomic fluorine:

$$Cl_2 + F \xrightarrow{k_{25}} ClF + Cl \ . \qquad (25)$$

Atomic chlorine product (Cl) can react with the reactor walls or with another gaseous constituent of the reaction mixture, or two atoms of Cl can recombine in a three-body collision with an energy acceptor:

$$Cl + Cl + M \xrightarrow{k_{26}} Cl_2 + M \ . \qquad (26)$$

In a qualitative experiment, a mixture of ~75 torr each of UF_6 and Cl_2 were irradiated with 266-nm wavelength light from a Nd:YAG laser (frequency quadrupled). (The reported UV-absorption cross-sections for UF_6, Cl_2, and ClF are presented in Fig. 7.) The 6-cm cubic irradiation cell had sapphire windows at two opposing faces to transmit UV radiation and silver chloride windows mounted orthogonally to permit IR scanning of the cell contents. Subsequent to UV irradiation, the IR spectrum indicated a loss of UF_6 (as monitored at 1160 and at 1290 cm^{-1}), and new absorption bands concurrently appeared at 760 and 785 cm^{-1}, characteristic of ClF [see Eq. (25) and Fig. 8].

Some solid residue appeared on the cell windows; the cell was evacuated, and the nonvolatile residue remaining on the windows was scanned to reveal absorption bands at approximately 620 and 560 cm^{-1}, and a strong absorption feature at lower wavenumbers. An in-house reference spectrum for β-UF_5 displayed absorption features at ~625, 570, and 430 cm^{-1}, whereas Jacob (1973) reports the spectrum of β-UF_5 to contain features at ~605, 573, and 512 cm^{-1}, with a broad band at 390 cm^{-1}. It appears probable that the nonvolatile residue in our photolysis experiment was β-UF_5 condensation product, similar to that reported by Lewis et al. (1979).

Attempts at quantitative estimates of the quantum yield [see Eq. (21)] for photolysis of UF_6 (reactant) in the presence of Cl_2, based on laser diode detection of ClF as the indicator species for UF_6 dissociation, produced values of ~2 (i.e., ~2 moles of ClF were formed per Einstein of radiation absorbed by UF_6 at wavelengths of 266 and 355 nm). (A more precise estimate of the quantum yield was hampered by the modest

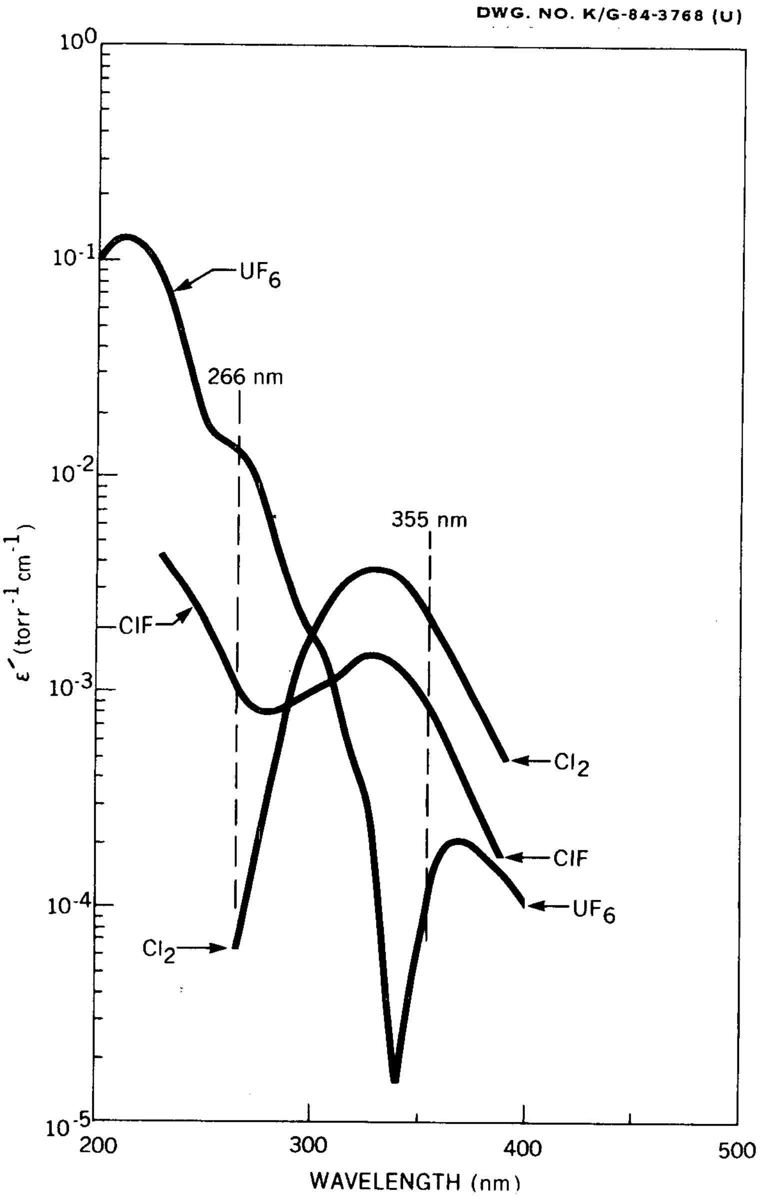

Fit. 7. UV-absorption cross-sections (ϵ', torr^{-1}, cm^{-1} for UF_6, Cl_2, and ClF).

DWG. NO. K/G-87-367 (U)

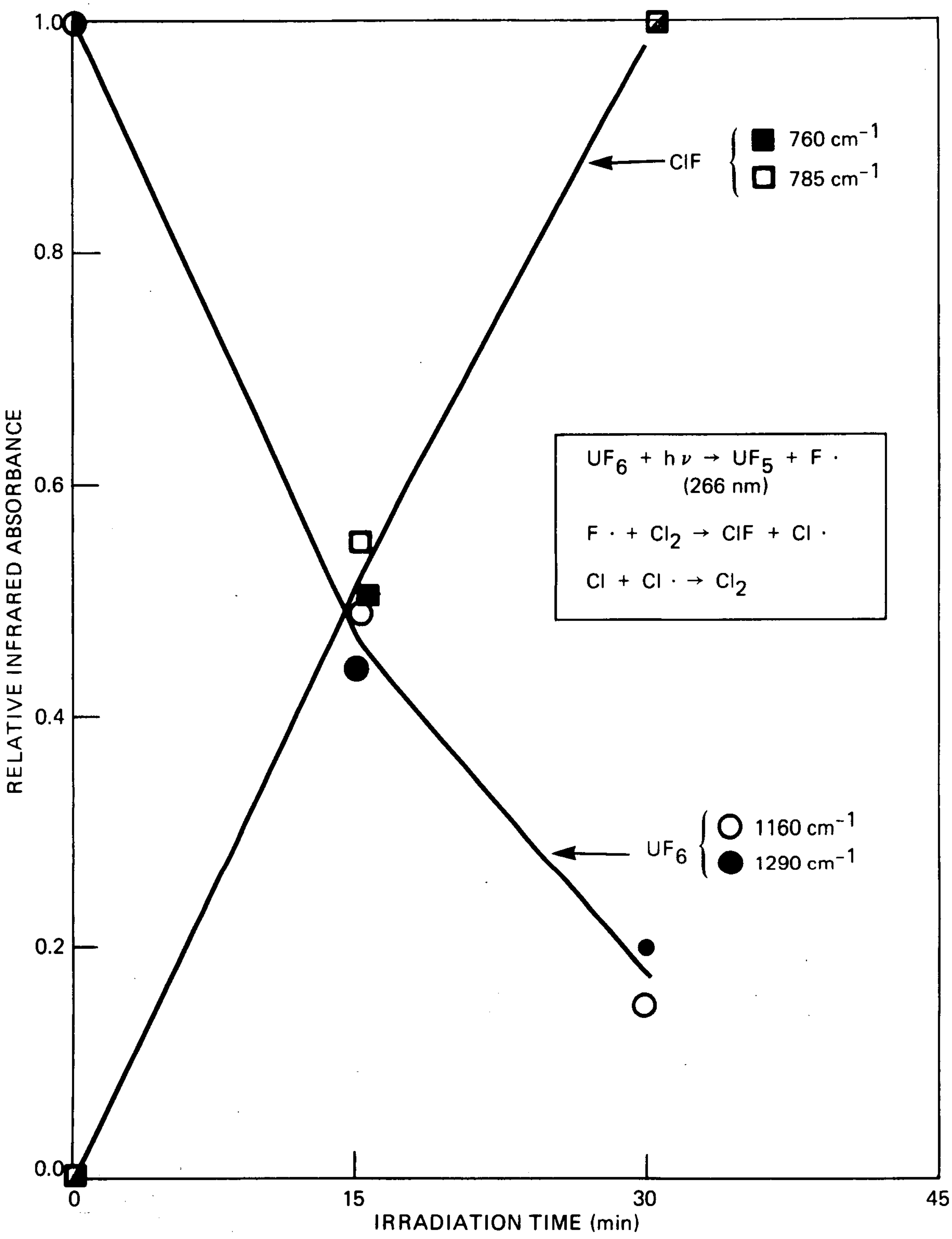

Fig. 8. Relative change in IR absorbance by UF_6 and ClF during photolysis of a mixture of UF_6 and Cl_2 at 266 nm.

stability of dilute ClF used as a calibration standard.) An apparent UV-photolysis quantum yield greater than unity suggests that atomic chlorine (produced by the photolysis of Cl_2 reagent) may react directly with UF_6:

$$UF_6 + Cl \rightarrow UF_5 + ClF \qquad (\Delta H_{298} = 8.2 \text{ kcal/mol}) \ . \qquad (27)$$

Reaction (27) is only slightly endothermic at room temperature and may become energetically favorable at elevated temperature or when UF_6 is in a vibrationally excited state.

We attempted a few semiquantitative UF_6 thermal dissociation studies using Cl_2 reagent. Detectable amounts of ClF were generated in the LPHP experiment, using SiF_4 as the sensitizer. Yields of ClF appeared to be higher than expected and somewhat erratic. We felt that this may be due to the ready thermolysis of Cl_2 reagent [see Eq. (28)] during the experiment (see Table 2: both Cl_2 and ClF bond dissociation energies are nearly 10 kcal more labile than the F-UF_5 bond), and the subsequent reaction [see Eq. (27)] between the atomic chlorine radical and UF_6.

$$Cl_2 + M \xrightarrow{k_{28}} Cl + Cl + M \ . \qquad (28)$$

We sought a trapping agent which would be effective at elevated temperature and which itself would be thermally stable. One attractive candidate is CF_3Cl (Freon 13). Homann and MacLean (1971) propose an energetically favorable fluorine atom substitution reaction in a sequence observed using a fluorine flame near 2000 K:

$$F + CF_3Cl \xrightarrow{k_{29}} CF_4 + Cl \qquad (\Delta H_{298} = -44.8 \text{ kcal}) \ . \qquad (29)$$

Both CF_3Cl and CF_4 are thermally stabile (see Table 2). The indicator species, CF_4, is easily detected by IR spectroscopy, with a sensitivity ~400 times that for IR detection of ClF product. Again, it is possible for Cl coproduct to subsequently react with UF_6 [see Eq. (27)], but this does not generate additional CF_4 indicator, and because only small fractional decompositions (<2%) of UF_6 are needed, this would not significantly alter the UF_6 concentration.

The reaction of F atoms with compounds of the series CF(x)Cl(4-x) results in abstraction of a Cl atom at room temperature and replacement of a Cl atom at flame temperatures (Jones and Skolnik, 1976). Foon (1972, 1975) proposed a different mechanism for the reaction between atomic fluorine and CF_3Cl at lower temperatures:

$$F + CF_3Cl \xrightarrow{k_{30}} ClF + CF_3 \qquad (\Delta H_{298} = -79.9\ \text{kcal})\ . \tag{30}$$

$$R\text{-}F + CF_3\cdot \rightarrow R + CF_4\ . \tag{31}$$

For abstraction from UF_6, Eq. (31) becomes

$$UF_6 + CF_3\cdot \rightarrow UF_5 + CF_4 \qquad (\Delta H_{298} = -56.8\ \text{kcal})\ , \tag{32}$$

which is energetically less favorable than $CF_3\cdot$ radical combination:

$$CF_3\cdot + CF_3\cdot \rightarrow C_2F6 \qquad (\Delta H_{298} = -82\ \text{kcal})\ . \tag{33}$$

Although Eq. (30) is energetically favorable, it may be slow kinetically. Zetzsch (1971) reacted atomic fluorine (generated from a microwave discharge) with several halogenated methanes (including CF_3Cl), yielding an upper estimate of the rate constant at 300 K of 1E9 cm^3/mol-s. Foon made indirect, relative rate measurements for a series of halogenated methanes with molecular fluorine and from rate ratios and thermodynamic theory, estimated the Arrhenius parameters for the rate constant for Eq. (30):

$$k_{30} = 6E13\ \exp(-20.9\ \text{kcal mol}^{-1}/RT)\ \text{cm}^3/\text{mol-s}\ . \tag{34}$$

At 300 K, Eq. (34) yields k_{30} = 0.04 cm^3/mol-s (vs the Zetzsch estimate of 1E9 cm^3/mol-s; see also Table 7). There were enough uncertainties in the derivation of Eq. (34) to question its usefulness for the prediction of absolute reaction rate, but it does suggest that there is an appreciable activation barrier to the reaction.

We attempted a room-temperature UV photolysis of UF_6 in CF_3Cl diluent, with IR monitoring for both CF_4 and ClF product. Almost no indicator species of either kind were formed; this may confirm that the room-temperature reaction between CF_3Cl and F is indeed slow, relative to UF_5 + F recombination. Alternately, the poor UV-photolysis quantum yield may have been due to the effectiveness of halomethanes as collision partners in quenching photolytically excited UF_6 prior to dissociation [Wampler (1979)].

Silicon tetrafluoride-sensitized laser pyrolysis of dilute UF_6 (at ~1350 K) in the presence of CF_3Cl produced very different results, as indicated in the IR scans illustrated in Fig. 9. During pyrolysis, UF_6 absorbance decreases, with a concurrent increase in CF_4 absorbance;

DWG. NO. K/G-87-368 (U)

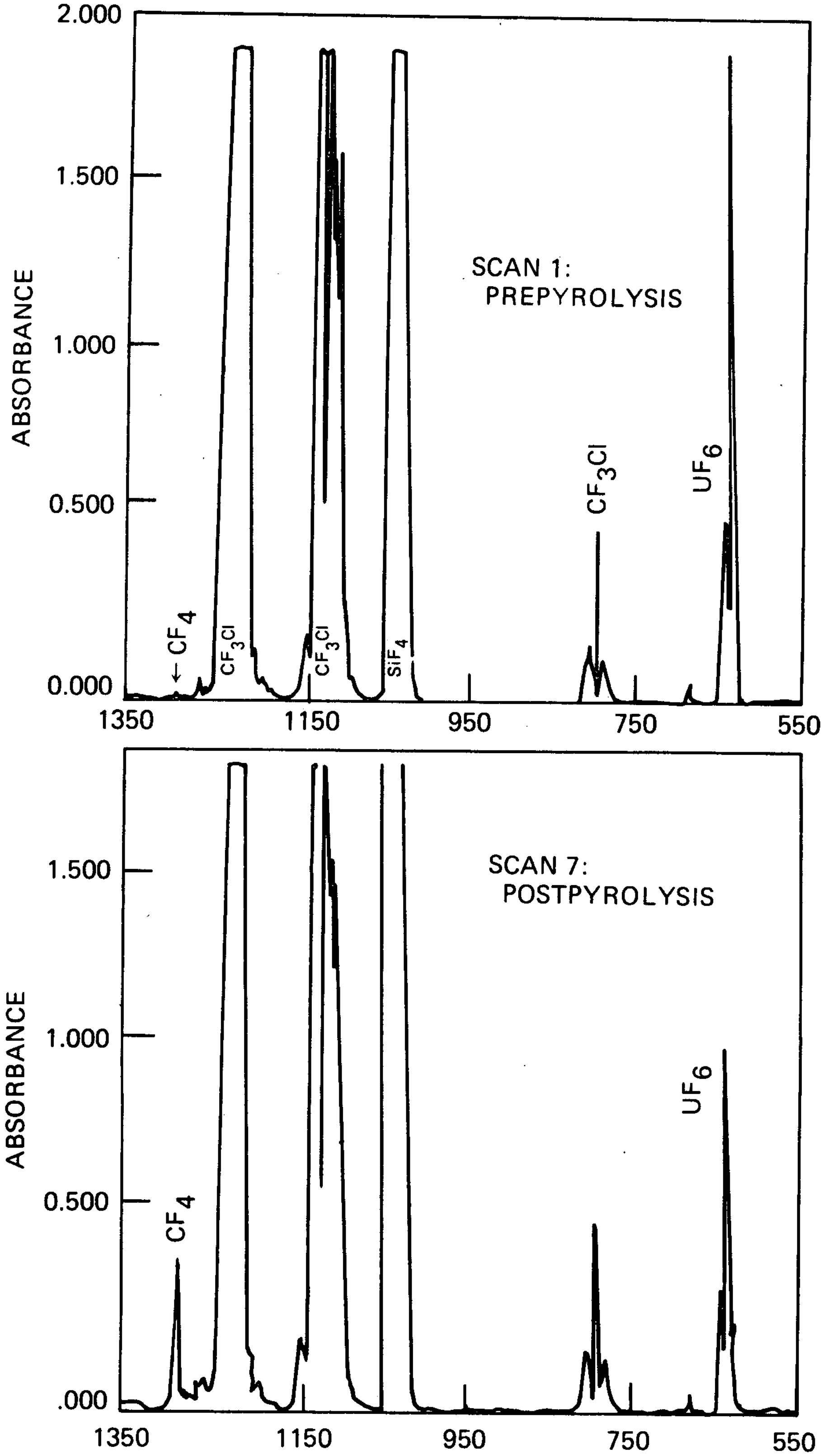

Fig. 9. FTIR scans of a mixture of gases with the initial room-temperature composition: UF_6 (1 torr), N_2 (4 torr), CF_3Cl (10 torr), and SiF_4 (15 torr). Scan 1 was taken before pulsed laser excitation, and scan 7 was taken after 120 laser pulses.

there is no evidence for C_2F_6 [see Eq. (33)], which absorbs very strongly in the monitored spectral region [Nielson et al. (1948)]; this is evidence that the F-atom substitution mechanism [see Eq. (29)] prevails at relatively high temperatures over the abstraction mechanism [see Eqs. (30-31) and (33)]. Additionally, the production of CF_4 was almost stoichiometric with respect to net UF_6 disappearence during pyrolysis (product yield ratio, 0.9 ± 0.2), indicating that for each mole of UF_6 which decomposes unimolecularly and which is not reformed by UF_5 + F recombination, one mole of CF_4 indicator is produced.

LPHP OF UF_6 WITH SIF_4 SENSITIZER AND CF_3Cl REAGENT

Quantitative measurements were performed with the cell geometry shown in Fig. 3B using the gas compositions given in Table 3. Ethyl chloride was used as the thermometer gas in an external standard; approximate temperature estimates for individual data points were derived using Eq. (11), assuming an effective reaction time of 20 µs and using the Holbrook and Marsh values (see Table 5) for As and Es at the high-pressure limit. [Note: varying the estimate of effective reaction time will correspondingly alter the estimate of effective temperature for individual data but will not significantly affect the values of the derived Arrhenius parameters; see McMillen et al. (1982).] The derived rate-temperature data parameters are given in Table 8, and the Arrhenius parameters derived from these data are summarized in Table 9.

Data were obtained over a range of total gas densities, using CF_3Cl as the diluent gas. The reason for this is twofold: first, an increase in atomic fluorine trapping reagent helps to ensure that, by mass-action, the formation of CF_4 product significantly outcompetes UF_5 + F recombination, and second, to ensure that the thermometer gas is sufficiently near its high-pressure-limiting rate to yield accurate estimates of the high-pressure-limiting rate for the reactant gas [Dai et al. (1982)].

A preliminary chemical dynamic modeling of our experiment at the lowest CF_3Cl and total densities used (see Table 2, data set A) was performed by J. L. Lyman (personal communication, March 1985); it was suggested that the CF_4 yield could represent as little as 65% of the total unimolecular dissociation under these conditions. (Note: these estimates were based on use of Eq. (34) for the rate of CF_3Cl + F reaction, and assumed an irreversible gas expansion model for the laser-induced shock wave; a reversible expansion model, with or without more rapid indicator reaction kinetics, would result in a higher estimate of CF_4 yield relative to total UF_6 unimolecular dissociation.) A significant contribution by UF_5 + F recombination in data set A (see Table 2) would have the effect of producing a lower estimate for log A (see Table 9).

In data sets C and D (see Table 8), the total concentration of CF_3Cl reagent is ~10 times that used in data set A, and the CF_4 yields in

Table 8. Laser-powered homogeneous pyrolysis of UF_6 – data summary

Data ID	Total gas density (mol/cm³)	UF_6 mol fraction	Derived kinetic parameters	
			T(K)[a]	k_u (s^{-1})
A(1-3)	1.67E-6	0.033	1346(±8)	(2.35 ± 0.35) E3
A-4	1.67E-6	0.158	1324	882
A-5	1.61E-6	0.167	1315	1450
A-6	1.61E-6	0.167	1288	940
A-7	1.64E-6	0.164	1223	108
A-8	1.61E-6	0.167	1218	258
A-9	1.61E-6	0.167	1190	74.2
A-10	1.61E-6	0.167	1150	18.8
A-11	1.64E-6	0.148	1114	23.4
A-12	1.61E-6	0.167	1105	7.6
B-1	4.04E-6	0.133	1211	594
B-2	4.14E-6	0.130	1199	501
B-3	4.09E-6	0.132	1117	58.5
B-4	4.11E-6	0.131	1107	48.4
C-1	7.64E-6	0.070	1163	426
C-2	6.62E-6	0.081	1160	424
C-3	6.73E-6	0.080	1098	84
C-4	6.73E-6	0.080	1051	17.4
D-1	8.07E-6	0.067	1098	56.4
D-2	8.07E-6	0.067	1096	64.9

[a] See Eq. (11); effective reaction time assumed to be 2E-5 s.

these experiments would be expected to be equivalent to the total UF_6 unimolecular dissociation. Pooling data from data sets C and D (total gas densities 6.7E-6 to 8.0E-6 mol/cm; see Table 8) yields the following estimate by our technique for the unimolecular decay rate for UF_6 near the high-pressure limit:

$$\text{Log } k_u \sim \text{Log } k_\infty = (16.04 \pm 0.9) - (71.3 \pm 4.4) \text{ kcal mol}^{-1}/2.3 \text{ RT} , \quad (35)$$

which is nearly identical to the high-pressure limit estimated from the Schug and Wagner data (see Table 10).

In summary, the LPHP and the shock tube techniques agree within experimental error near the high-pressure limit. However, due to the relative rate procedure used in the LPHP technique, it does not necessarily give a true representation of the pressure-dependent rate falloff for the reactant gas; rather, the Arrhenius parameters estimated using Eq. (11) tend to be closer to the high-pressure limit than to the absolute rate constants at a given gas density.

Table 9. Laser-powered homogeneous pyrolysis of UF_6 - derived Arrhenius parameters

Data set[a]	Total gas density (mol/cm^3)	Log k_u = Log A - eA/2.3RT	
		Log A	Ea (kcal/mol)
A	1.6E-6	14.15 ±0.7	66.6 ±0.9
B	4.0E-6	14.76 ±0.4	66.3 ±1.9
C	6.7E-6	15.70 ±0.5	69.4 ±2.3
C + D	(6.7-8.0) E-6	16.04 ±0.9	71.3 ±4.4

[a] See Table 2.

Table 10. Estimates of the high-pressure limiting Arrhenius parameters for UF_6 thermal dissociation

Experimental data set[a]	Eq. no.	Extrapolation procedure	Log k_∞ = Log A -Ea/2.3RT		
			Log A	Ea (kcal/mol)	Log K (1200 K)
S and W	(8)	Kassel theory	16.52 (±0.7)	70.3 (±4)	3.718
	(9)	Empirical	16.04 (±0.3)	67.8 (±2)	3.700
	(10)	RRKM	16.42	69.7	3.727
LPHP	(35)	Relative rate	16.04 (±0.9)	71.3 (±4)	3.056

[a] S and W = data from Schug and Wagner (1977). LPHP = data from this work.

ACKNOWLEDGMENTS

We would like to thank Dr. John L. Lyman of the Los Alamos National Laboratory for his many valuable suggestions during the course of this work and for his making available to us some unpublished RRKM model rate predictions. We also thank Dr. Myron Kaufman of Emory University for his consultation during the initial stages of this work concerning the reactions of atomic fluorine.

REFERENCES

Andreoni, A. et al. (1980), "Near-UV photodissociation of gaseous uranium hexafluoride in the presence of molecular hydrogen," *Chem. Phys. Lett.*, **69**, 161.

Angelie, C., Cauchetier, M., and Paris, J. (1982), "Sensitized dissociation of UF_6, $XeOF_4$, and SF_5Cl by SF_6 excited with a pulsed CO_2 laser," *Chem. Phys.*, **66**, 129.

Asaba, T., Yoneda, K., and Hikita, T. (1962), "Shock-tube studies on the pyrolysis of lower hydrocarbons. III. Shock-tube study of the high temperature pyrolysis of ethylene", *Kogyo Kagaku Zasshi*, **65**, 1811 (*Chem. Abstr.*, **59**:1461g).

Bacher, W. and Jacob, E. (1982), "Uranhexafluorid-chemie und technologie eines grundstoffs des nuklearen brennstoff-kreislaufes," *Chem.-Zeitung*, **106**, 117.

Barber, E. J. (1985), "The thermodynamics and kinetic modeling of the reduction of uranium hexafluoride to uranium tetrafluoride by hydrogen," K/PS-1127, Martin Marietta Energy Systems, Inc., Oak Ridge Gaseous Diffusion Plant.

Barnard, J. A., Cocks, A. T., and Lee, R. K-Y (1974), "Kinetics of the Thermal Unimolecular Reactions of Cyclopropane and Cyclobutane Behind Reflected Shock Waves," *J. Chem. Soc., Faraday Trans. 1*, **70**, 1782.

Baulch, D. L. et al. (1981), "Evaluated kinetic data for high temperature reactions. Vol. 4: Homogeneous gas phase reactions of halogen- and cyanide-containing species," *J. Phys. Chem. Ref. Data*, **10**, (Suppl. no. 1).

Belford, R. L. and Strehlow, R. A. (1969), "Shock tube technique in chemical kinetics", pp. 247-272, in *Annual Rev. Phys. Chem.*, Vol. 20, eds. H. Eyring, C. J. Christensen, and H. S. Johnston.

Benson, S. W. and O'Neal, H. E. (1970), "Kinetic Data on Gas Phase Unimolecular Reactions," NSRD-NBS 21.

Boyd, M. L., Wu, T-M, and Back, M. H. (1968), "Kinetics of the thermal reactions of ethylene. Part I," *Can. J. Chem.*, **46**, 2415.

Chambers, T. S. and Kistiakowsky, G. B. (1934), "Kinetics of the thermal isomerization of cyclopropane," *J. Amer. Chem. Soc.*, **56**, 399.

Comita, P. B. et. al. (1981), "Laser-powered homogeneous dissociation of tetralin," *J. Phys. Chem.*, **85**, 3266.

Compton, R. N. (1977), "On the formation of positive and negative ions in gaseous UF_6," *J. Chem. Phys.*, **66**, 4478.

Cottrell, T. L. and McCoubrey, J. C. (1961), "*Molecular Energy Transfer in Gases*, Butterworths, London.

Cravens, D., Shields, F. D., and Bass, H. E. (1979), "Vibrational Relaxation of UF_6: Ultrasonic Measurements in Mixtures with Ar and N_2," *J. Chem. Phys.*, **71**, 2797.

CRC Handbook of Chemistry and Physics (1985), 66th ed., CRC Press, Inc., West Palm Beach, Florida.

Dai, H. L., Specht, E., Berman, M. R., and Moore, C. B. (1982), "Determination of Arrhenius parameters for unimolecular reactions of chloroalkanes by IR laser pyrolysis," *J. Chem. Phys.*, **77**, 4494.

Danen, W. C. and Jang, J. C. (1981), "Multiphoton infrared excitation and reaction of organic compounds," pp. 45-164 in *Laser-Induced Chemical Processes*, ed. J. I. Steinfeld, Plenum Press, New York.

Delliste, D., Richard, C., and Martin, R. (1981), "La reaction thermique de l'ethylene vers 500°C: modelisation au cours du temps et determination de constants de vitess," *J. Chim. Phys.*, **78**, 655.

Dillman, B. and Heydtmann, H. (1977), "Application of Forst's method to the calculation of thermal unimolecular reaction rates and isotope effects in the falloff region," *Int. J. Chem. Kinet.*, **9**, 321.

Emanuel, G. (1969), "Table of the Kassel Integral," Air Force Report No. SAMSO-TR-69-36, Aerospace Report No. TR-0200(4240-20)-5.

Emanuel, G. (1972), "Table of the Kassel Integral," *Int. J. Kinet.*, **4**, 591.

Evans, P. J., Ichimura, T. and Tschuikow-Roux, E. (1978), "A comparison of two single-pulse shock-tube techniques: the thermal decomposition of ethyl chloride and n-propyl chloride," *Int. J. Chem. Kinet.*, **10**, 855.

Farneth, W. E. et al. (1976), "Time resolved infrared laser photochemistry and spectroscopy: the methyl fluoride sensitized decomposition of tetramethyl-1,2-dioxetane. An example of infrared laser induced electronic excitation," *J. Amer. Chem. Soc.*, **98**, 7877.

Foon, R. and Kaufman, M. (1975), "Kinetics of gaseous fluorine reactions," in *Progress in Reaction Kinetics*, Vol, 8, Pt. 2, eds. K. R. Jennings and R. B. Cundall.

Foon, R. and Tait, K. B. (1972), "Chlorine abstraction reactions of fluorine. 3. Thermochemical date for chlorofluoroalkanes," *J. Chem. Soc.*, Faraday Trans. **68**, 1121.

Furue, H. and Pacey, P. D. (1982), "The Pressure Dependence of the Rate of Isomerization of Cyclopropane at 897K," *Can. J. Chem.*, **60**, 916.

Galkin, N. P. and Tumanov, Y. N. (1971), *Atomnaya Energiya*, **30**, 372 (*Chem. Abstr.*, **75**: 91690n).

Glanzer, K. and Troe, J. (1972), "Thermische Zerfallreaktionen Von Nitroverbindungen I. Dissoziation Von Nitromethan," *Helv. Chim. Acta*, **55**, 2884.

Golden, D. M., Solly, R. K., and Benson, S. W. (1971), "A Comparison of RRK and RRKM Theories for Thermal Unimolecular Processes," *J. Phys. Chem.*, **75**, 1333.

Hassan, H. A. and Deese, J. E. (1974), "Thermodynamic properties of UF_6 at high temperatures," Report NASA-CR-2373.

Heydtmann, H., Dill, B., and Jonas, R. (1975), "The thermal unimolecular decompositions of C_2H_5Cl, i-C_3H_7Cl, and t-C_4H_9Cl," *Int. J. Chem. Kinet.*, **7**, 973.

Hildenbrand, D. L. (1977),"Thermochemistry of gaseous uranium pentafluoride and uranium tetrafluoride," *J. Chem. Phys.*, **66**, 4788.

Holbrook, K. A. and Marsh, A. R. W. (1967), "Unimolecular gas-phase pyrolysis of ethyl chloride," *Trans. Faraday Soc.*, **63**, 643.

Homann, K. H. and MacLean, D. I. (1971), "Structure of fluorine-supported flames. I. Method of investigation. The Dichlorodifluoromethane-fluorine flame," *J. Phys. Chem.*, **75**, 3645.

Howlett, K. E. (1952), "Studies on unimolecular chlorohydrocarbon decompositions, Part III," *J. Chem. Soc.*, 4487.

Jacob, E. (1973), "Contributions to the chemistry of the uranium fluorides and oxyfluorides. II. The preparation and vibrational spectra of alpha- and beta-uranium pentafluorides," *Z. Anorg. Allgemein Chemie*, **400**, 45 (*Chem. Abstr.* **83**: 52497a).

Jasinski, J. M, and Estes, R. D. (1985), "Laser powered homogeneous pyrolysis of silane," *Chem. Phys. Lett.*, **117**, 495.

Jones, W. E. and Skolnik, E. G. (1976), "Reactions of fluorine atoms," *Chem. Rev.*, **76**, 563.

Karve, R. S. et al. (1981), "Sensitized multiphoton dissociation of UF_6 in SF_6-UF_6 mixtures," *Chem. Phys. Lett.*, **78**, 273.

Kassel, L. S. (1932), The Kinetics of Homogeneous Gas Reactions, American Chemical Society Monograph Series, Vol. 57, Chemical Catalog Company, Inc., New York.

Kozlov, G. I. and Knorre, V. G. (1964), "Kinetic study of thermal decomposition of some hydrocarbons (acetylene, ethylene, ethane and methane) by single shock wave," Ispol'z. Tverd. Topliv, Sernistykh

Mazutov i Gaza, Akad. Nauk SSSR, Energ. Inst. No. 5, 157) (*Chem. Abstr.* **62**:16016d).

Laidler, K. J. (1965), *Chemical Kinetics*, 2nd ed., McGraw-HillBook Co., New York.

Lambert, J. D. (1977), *Vibrational and Rotational Relaxation in Gases*, Clarendon Press, Oxford.

Lau, K. H. and Hildenbrand, D. L. (1982), "Thermochemical properties of the gaseous lower valent fluorides of uranium," *J. Chem. Phys.*, **76**, 2646.

Leitnaker, J. M. (1983), "Thermodynamic data for uranium fluorides," K/PS-352, Martin Marietta Energy Systems, Inc., Oak Ridge Gaseous Diffusion Plant.

Lewis, D. K., Giesler, S. E., and Brown, M. S. (1978), "Further Study of Cyclopropane Structural Isomerization Behind Reflected Shock Waves," *Int. J. Chem. Kinet.*, **10**, 277.

Lewis, K. E., McMillen, D. F., and Golden, D. M. (1980), "Laser-powered homogeneous pyrolysis of aromatic nitro compounds," *J. Phys. Chem.*, **84**, 226.

Lewis, W. B., Wampler, F. B., Huber, E. J., and Fitzgibbon, G. C. (1979), "Photolysis of uranium hexafluoride and some reaction variables affecting the apparent quantum yield," *J. Photochem.*, **11**, 393.

Lyman, J. L. (1977), "A model for unimolecular reaction of sulfur hexafluoride," *J. Chem. Phys.*, **67**, 1868.

Lyman, J. L., Laguna, G., and Greiner, N. R. (1985), "Reactions of uranium hexafluoride photolysis products," *J. Chem. Phys.*, **82**, 175.

Lyman, J. L. and Holland, R. (1985), Los Alamos National Laboratory, Los Alamos, New Mexico, personal communication to W. D. Bostick, Martin Marietta Energy Systems, Inc., Oak Ridge, Tennessee.

McMillen, D. F. et al. (1982), "Laser-powered homogeneous pyrolysis. Thermal studies under homogeneous conditions, validation of the technique, and application to the mechanism of azo compound decomposition," *J. Phys. Chem.*, **86**, 709.

Mulcahy, M. F. R. (1973), *Gas Kinetics*, John Wiley and Sons, New York.

Myerson, A. L. and Chuldzinski, J. J. (1981), "Chemical kinetics of the gas-phase reaction between uranium hexafluoride and hydrogen," *J. Phys. Chem.*, **85**, 3905.

Nazarov, E. K. and Torban, B. S. (1966), "Kinetics of high-temperature pyrolysis of individual hydrocarbons," *Inform. Soobshch. Gos. Nauch.-Issled. Proekt. Inst. Azotn. Prom. Prod. Org. Sin.* **17**, 53 (*Chem. Abstr.* **68**:113838b)

Nielson, J. R., Richards, C. M., and McMurry, H. L. (1948), "The infra-red absorption spectrum of hexafluoroethane gas," *J. Chem. Phys.*, **16**, 67.

Olszyna, K. J., Grunwald, E., Keehn, P. M, and Anderson, S. P. (1977), "Megawatt infrared laser chemistry. II. Use of SiF_4 as an inert sensitizer," *Tetrahedron Lett.*, 1609.

Oref, I. and Rabinovitch, B. S. (1968), "The experimental evaluation of k_∞ in unimolecular reaction systems," *J. Phys. Chem.*, **72**, 4488.

Pritchard, H. O., Snowden, R. G., and Trotman-Dickenson, A. F. (1953), "Studies in energy transfer. II. The isomerization of cyclopropane - a quasi-unimolecular reaction," *Proc. Roy. Soc. (London)*, **A217**, 563.

Rabek, J. F. (1982), *Experimental Methods in Photochemistry and Photophysics*, John Wiley and Sons, New York.

Rienäcker, K. (1981), "Kinetische untersuchungen von reaktionen des UF_6 in der gasphase," Ber.-Max Plank Inst. Stromungsforsch., 1 ("Kinetic investigations of UF_6 reactions in the gaseous phase," K/TR-86/15).

Robinson, P. J. and Holbrook, K. A. (1972), *Unimolecular Reactions*, Wiley-Interscience, New York.

Schranz, H. W., Nordholm, S., and Hamer, N. D. (1982), "Quantized RRK Theory of Unimolecular Reaction Rates," *Int. J. Chem. Kinet.*, **14**, 543.

Schug, K. P. and Wagner. G. (1977), Zum thermischen zerfall von UF_6 in der gasphase", *Z. Phys. Chem.*, **108**, 172. ("Thermal decomposition of UF_6 in the gas phase," ORNL/TR-86/11.)

Shaub, W. M. and Bauer, S. H. (1975), "Laser-powered homogeneous pyrolysis," *Int. J. Chem. Kinetics*, **7**, 509.

Skinner, G. B. and Sokoloski, E. M. (1960), "Shock tube experiments on the pyrolysis of ethylene," *J. Phys. Chem.*, **64**, 1028.

Skinner, G. B. and Rabinovitch, B. S. (1972), "Some Comparisons of the RRK and RRKM Theories of Thermal Unimolecular Reaction. Energy Distributions and the s Parameter," *J. Phys. Chem.*, **76**, 2418.

Smith, G. P. and Laine, R. M. (1981), "Organometallic bond dissociation energies. Laser pyrolysis of $Fe(CO)_5$," *J. Phys. Chem.*, **85**, 1620.

Steel, C. et al. (1979), "Chemical thermometers in megawatt infrared laser chemistry: the decomposition of cyclobutanone sensitized by ammonia," *Chem. Phys. Lett.*, **62**, 121.

Swope, L. (1971), "Heated infrared sample cell for volatile fluorides," *Rev. Sci. Instr.*, **42**, 1502.

Tardy, D. C. and Rabinovitch, B. S. (1968), "Collisional Energy Transfer in Thermal Unimolecular Systems. Dilution Effects and Falloff Region," *J. Chem. Phys.*, **48**, 1282.

Troe, J. and Wagner, H. G. (1967), "Unimolekulare Reactionen in Thermischen Systemen," *Berichte Buns.*, **71**, 937.

Troe, J. (1975), "Unimolecular reactions: experiments and theories," in *Physical Chemistry: An Advanced Treatise*, Vol. VIB/Kinetics of gas reactions, ed. W. Jost, Academic Press, New York.

Troe, J. (1979), "Predictive Possibilities of Unimolecular Rate Theory," *J. Phys. Chem.*, **83**, 114.

Trotman-Dickerson, A. F. (1955), *Gas Kinetics*, Academic Press, New York.

Tsang, W., Walker, J. A., and Braun, W. (1982), "Thermal, unsensitized infrared laser, and laser SiF_4 sensitized decomposition of 1,2-dichloropropane," *J. Phys. Chem.*, **86**, 719.

Tumanov, Y. N. (1968), "Thermodynamic stability of uranium hexafluoride," *Zh. Neorg. Khim.*, **13**, 1488 (ANL-Trans-738).

Tumanov, Y. N. and Galkin, N. P. (1972), "Mechanism of the hydrogen reduction of uranium hexafluoride," *At. Energ.*, **32**, 21 (*Chem. Abstr.*: **90570**g).

Wagman, D. D. et al. (1982), "The NBS Tables of Chemical Thermodynamic Properties," *J. Phys. Chem. Ref. Data*, **11** (Suppl. 2).

Walsh, R. (1981), "Bond dissociation energy values in silicon-containing compounds and some of their implications," *Accts. Chem. Res.*, **14**(8), 246.

Wampler, F. B., Oldenborg, R. C., and Rice, W. W. (1979), "Quenching of uranium hexafluoride (A state) by halomethanes," *J. Photochem.*, **11**, 379.

Warnatz, J., Wagner, H. G., and Zetzsh, C. (1971), "Determination of the rate of reaction of fluorine atoms with molecular chlorine," *Ber. Bunsenges. Phys. Chem.*, **75**, 119 (*Chem. Abstr.* **74**:103554r).

Yau, A. W. and Pritchard, H. O. (1978), "A reformation of the theory of unimolecular reactions," *Can. J. Chem.*, **56**, 1389.

Zetzch, C. (1971), "Untersuchungen des Reactionsverhaltens von F-atomen in der Gasphase," Ph.D. dissertation, Georg-August University, Gottingen, Germany.

APPENDIX

APPLICATION OF THE RICE-RAMSPERGER-KASSEL THEORY

The experimental techniques used in the main body of this document provide information primarily for the high-pressure limiting unimolecular decomposition rate for UF_6. In engineering applications, there is often a need for expedient estimates of reaction rates beyond the bounds of available experimental data, e.g., to differing regimes of temperature and pressure.

Unimolecular reaction rate theories have been studied for many decades. Techniques for estimating the fundamental behavior of unimolecular rates as a function of temperature, pressure, and intermolecular and intramolecular energy transfer characteristics are available at many levels of sophistication and ease of application. To our knowledge, all theoretical treatments, to the extent that they are applied to experimental data, use some degree of adjustable parameterization to best match the data [see Robinson and Holbrook (1972)]. The problem is thus to select a technique which provides a degree of theoretical validity and accuracy commensurate with the available data and the requirements for the application at hand.

For many applications, the Rice-Ramsperger-Kassel (RRK) theory provides a reasonable compromise. The classical formulation, as given in Mulcahy (1973), is

$$\frac{k_u}{(k_u)_\infty} = \frac{1}{(s-1)!}\int_0^\infty \frac{x^{s-1}\exp(-x)dx}{1 + A\{x/(x + E^*/RT)\}^{s-1}/\lambda Z[M]} , \qquad \text{(A-1)}$$

where

$x = (E - E^*)/RT$ is the integration variable,

E = total internal energy,

E^* = critical internal energy, approximately equal to Ea, the Arrhenius activation energy at the high-pressure limit,

A = Arrhenius pre-exponenial factor at the high-pressure limit,

Z = collision frequency for the reactant molecule,

$[M]$ = total gas concentration (e.g., molec/cm^3),

λ = "collision-effectiveness parameter,"

S = number of "effective oscillators."

The classical RRK formulation shown in Eq. (A-1) is an adaptation of an equivalent quantum mechanical formulation. Use of the classical version becomes invalid when the total internal vibrational energy becomes smaller than, or comparable in magnitude to, the energy of individual vibrational quanta. Vibrational frequencies for selected molecules are given in Table A-1. Consider the example of UF_6 (a seven-atom molecule) at a temperature near 1000 K: the classical average internal vibrational energy would thus be (3N-6)RT or ~30,000 cal/mol as compared with vibrational quanta averaging 286 cm^{-1} or ~818 cal/mol. For this example, the conditions for use of the classical formulation are well satisfied; however, this may not always be the case for systems such as hydrocarbons [higher mean vibrational frequencies (see Table A-1)] at significantly lower temperatures.

A computer program was written to evaluate this version of the classical RRK formula; a listing of the program, RRK.BAS, is given in Fig. A-1. The main function of the program is to numerically integrate the RRK integral described previously and to calculate the ratio of the unimolecular rate constant to the high-pressure limiting rate constant at otherwise equivalent conditions.

For our purposes, speed and ease of implementation are more important than high precision, and, therefore, numerical integration is achieved to adequate accuracy using the trapezoidal rule. The integration interval is taken as (dx = 0.1); in numerous test cases, the integrand result converged for all values of dx below 0.5. The RRK integral, as written in Eq. (A-1), is for a semi-infinite range. The integrand, however, diminishes for large values of x, so that in practice, the integration may be terminated at finite (x) without loss of precision. In the program, the integration is terminated when two criteria are met: (1) the integrand is falling in value, and (2) the value of the current increment of the integral is less than one part in 10^6 of the cumulative integral. The choices of (dx) and the convergence criteria are encoded into the program but are easily changed.

In the evaluation of factorials in the integral, Stirling's approximation is used; namely,

$$S! \sim \sqrt{2\pi S}\,(S/e)^S \ . \qquad \text{(A-2)}$$

While this approximation is not terribly accurate for small values of S, it has the advantage of easily permitting computation of factorials for fractional numbers and is sufficiently precise for values of S considered in this study.

The values for the RRK integral computed using the program listed in Fig. A-1 compare well with the standard values computed and compiled by Emanuel (1969, 1972); note that use of the standard tables is slow and typically requires interpolation for use with real systems. [Some notes on the use of Fig. A-1: (1) RRK.BAS is written for the IBM PC in BASICA; when compiled using the 8087 coprocessor, it runs in ~1 s, whereas the

Table A-1. Some physical parameters for selected molecules

Molecule	Molecular weight	Collision diameter (A)[a]	Fundamental vibrational frequencies (cm^{-1})[b]
Argon	39.95	3.54	
cyclo-C_3H_6	42.1	4.81	$\nu_1 = 3038$, $\nu_2 = 1479$, $\nu_3 = 1188$, $\nu_4 = 1126$, $\nu_5 = 1070$, $\nu_6 = 3103$, $\nu_7(2) = 854$, $\nu_8(2) = 3025$, $\nu_9(2) = 1438$, $\nu_{10}(2) = 1029$, $\nu_{11}(2) = 866$, $\nu_{12}(2) = 3082$, $\nu_{13}(2) = 1188$, $\nu_{14}(2) = 739$ (geometric mean: 1432)
C_2H_5Cl	64.5	4.90	$\nu_1 = 2967$, $\nu_2 = 2946$, $\nu_3 = 2881$, $\nu_4 = 1463$, $\nu_5 = 1448$, $\nu_6 = 1385$, $\nu_7 = 1289$, $\nu_8 = 1081$, $\nu_9 = 974$, $\nu_{10} = 677$, $\nu_{11} = 336$, $\nu_{12} = 3014$, $\nu_{13} = 2986$, $\nu_{14} = 1448$, $\nu_{15} = 1251$, $\nu_{16} = 974$, $\nu_{17} = 786$, $\nu_{18} = 251$ (geometric mean: 1268)
SiF_4	104.1	4.88	$\nu_1 = 800$, $\nu_2(2) = 268$, $\nu_3(3) = 1032$, $\nu_4(3) = 389$ (geometric mean: 537)
CF_3Cl	104.5	4.86	$\nu_1 = 1106$, $\nu_2 = 782$, $\nu_3 = 474$, $\nu_4(2) = 1217$, $\nu_5(2) = 560$, $\nu_6(2) = 350$ (geometric mean: 659)
SF_6	146.1	5.13	$\nu_1 = 774$, $\nu_2(2) = 642$, $\nu_3(3) = 948$, $\nu_4(3) = 616$, $\nu_5(3) = 525$, $\nu_6(3) = 347$ (geometric mean: 592)
UF_6	352.0	5.97	$\nu_1 = 667$, $\nu_2(2) = 533$, $\nu_3(3) = 626$, $\nu_4(3) = 186$, $\nu_5(3) = 202$, $\nu_6(3) = 142$ (geometric mean: 286)

[a] Collision diameters (in Angstra) estimated from Lennard-Jones parameters.

[b] Parenthetic terms designate degeneracies.

```
10 ' RRK7      Numerical Integration of RRK integral from Mulcahey p 200
20 '                    LDT 6 Jun 85
30 GOSUB 410:GOSUB 200
40 DEF FNCTORIAL(X)=SQR(6.2838531#*X)*(X/2.71828183#)^X
50 DEF FNI(Y,F,T,C,EA)=Y^F*EXP(-Y)/(1+C*(Y/(Y+EA/T))^F)
60 DIM CUM(15)
70 GOSUB 330
80 X=0:I=0:CUM(S)=0
90 CUM(S)=FNI(DX,S-1,T,C,EA)/4*DX                    ' (f(0)+f(dx))/2)
100 I=I+1:X=X+DX
110 DC=FNI(X,S-1,T,C,EA)/FNCTORIAL(S-1)*DX
120 CUM(S)=CUM(S)+DC
130 IF I<20 OR DC*1000000!   >  CUM(S) THEN GOTO 100
140 PRINT
150 KPKI=CUM(S):PRINT USING
 "At    T = ##### K     P = ##### Torr    s = ###.# ";T,P,S
160 PRINT USING
 "Integral converges at #### iterations to K/
 Kinf = #.#####    log = ##.###";I,KPKI,LOG(KPKI)/2.302585
170 KU=KPKI*AO*EXP(-EA/T):PRINT USING
 "                                          Ku     =##.##^^^^   log = ##.###";
 KU,LOG(KU)/2.302585
180 PRINT:PRINT:GOTO 70
190 STOP
200 INPUT "Ea ( cal/mole)       ";EA:EA=EA/1.987    ' K
210 INPUT "Ao (1/sec)           ";AO
220 LAMBDA=1 '                         '"strong collision"
230                                    'c==Ao/(Lambda*Z*[A])
240 DX=.1                              'integration interval (.5 is max
                                        value giving limiting value)
250 INPUT "Reactant: Mass (amu) ";M1
260 INPUT "Reactant: Dia. (Ang) ";R1
270 INPUT "Self-medium (Y/N)    ";Q$:Q$=LEFT$(Q$,1):
      IF Q$="y" OR Q$="Y"THEN M2=M1:R2=R1:F=.5:GOTO 310
280 F=1                                ' statistical; .5 in self-media
290 INPUT "Diluent : Mass (amu) ";M2
300 INPUT "Diluent : Dia. (Ang) ";R2
310 MU=M1*M2/(M1+M2):SIGMA=1E-08*(R1+R2)/2
320 RETURN
330 INPUT "T(K)                 ";T
340 INPUT "Total Pressure (Torr)";P
350 INPUT "RRK S factor         ";S
360 V=SQR(8*8.314E+07*T/3.14159/MU)      ' cm/sec  - collision velocity
370 Z=3.14159*SIGMA*SIGMA*V*F            ' cc/molec-sec
380 N=P/760/82.05/T*6.02E+23             ' molec/cc
390 C=AO/Z/N/LAMBDA                      ' numeric constant
400 RETURN
410 CLS:PRINT"RRK Unimolecular Kinetics - Numerical Integration of
420     PRINT
 "                            RRK integral from Mulcahy p 201"
430 PRINT
440 RETURN
```

Fig. A-1. Listing of RRK.BAS.

interpreted version (i.e., as run directly from BASICA) requires ~30 s; (2) several lines exceed the paper width in Fig. A-1 and are continued on the next line (e.g., line 150); and (3) the collision-efficiency parameter (λ) is set equal to 1 in line 220 but can easily be altered or treated as an input variable.]

A sample of the CRT screen output from execution of RRK.BAS (see Fig. A-1) is given in Fig. A-2. In this example, the input high-pressure Arrhenius parameters for UF_6 were taken from Eq. (8) of the main text, and the values for reactant mass and diameter were selected from Table A-1.

PARAMETERIZATION OF THE RRK MODEL

The RRK theory provides a (relatively) simple technique for estimating the pressure-dependent fall-off in unimolecular reaction rates. Given the high-pressure Arrhenius rate parameters and selected fundamental physical properties of the molecules comprising the system, RRK can be used to fit experimental data with 0, 1, or 2 adjustable parameters (S_{eff} and λ).

The Arrhenius parameters for the high-pressure limiting rate are generally obtained from the experimental data or derived via techniques such as described in the main text of this report. The collision frequency, Z, derived from the gas kinetic hard-sphere collision rate, is a function of gas component molecular weight, collision diameter, and temperature; some parameters used in computing Z for selected collision partners are summarized in Table A-1. The total gas composition and concentration affects the rates for activation and deactivation of reactant [see Eq. (4) of the main text].

The term λ is an accommodation coefficient equal to the fraction of collisions of the activated species which result in deactivation; generally, for lack of other information, λ is assumed to be unity in self-medium ("strong collision" approximation). Following this convention, λ thus becomes a measure of "relative collision efficiency," analogous to the β_c term defined by Tardy and Rabinovitch (1968) and can assume values ranging from near zero (for inefficient deactivation--as in V-T energy transfer by "weak" collisions with inert gases) to values near unity (for "strong" collisions with polyatomic molecules, with many vibrational modes, where efficient, near-resonant V-V energy transfer is possible). In practice, one method of obtaining information on the rates of energy transfer between molecules is to study the efficiency of chemically inert gases in maintaining the rate of unimolecular reactions near the low-pressure rate limiting domain [Holbrook (1955), Cottrell and McCourbey (1961)]. In general, it appears that efficiency of energy transfer increases with increasing complexity of the collision partner but that a maximum efficiency (comparable to self-medium) is soon reached; in contrast, the smaller and lighter molecules are very inefficient, in spite of their known efficiency as collision partners for V-T energy transfer.

```
------------------------------------------

RRK Unimolecular Kinetics - Numerical Integration of
                            RRK integral from Mulcahy p 201

Ea ( cal/mole)        ? 70300
Ao (1/sec)            ? 3.3e16
Reactant: Mass (amu) ? 352
Reactant: Dia. (Ang) ? 6.0
Self-medium (Y/N)     ? y
T(K)                  ? 1000
Total Pressure (Torr)? 50
RRK S factor          ? 12

At     T =  1000 K     P =    50 Torr    s =  12.0
Integral converges at  212 iterations to K/Kinf = 0.09234   log = -1.035
                                         Ku     = 1.31E+00  log =  0.119
-----------------------------------------------------------------------
```

Fig. A-2. Sample screen output of RRK.BAS.

From this, Lambert (1977) infers that V-T energy transfer does not play an important role in unimolecular reactions.

When the "strong collision" assumption is invoked for unimolecular reactions in self-medium or in a polyatomic bath gas (i.e., $\lambda = 1$), the primary remaining adjustable parameter in the RRK model is S_{eff}, the *number of* "effective oscillators" in the reactant molecule, or loosely the number of internal vibrational modes which participate in distributing internal molecular energy. It can have values ranging up to the total 3N-6 vibrational degrees of freedom for the (nonlinear) N-atom polyatomic reactant. S_{eff} can be treated as an adjustable parameter to provide best agreement with the available experimental data, and frequently it is thus found to be about one-half of the total number of oscillators [Laidler (1965)] or a somewhat larger fraction for highly symmetric molecules. From quantum and statistical mechanical considerations, one might expect S_{eff} to have some dependence on temperature and internal vibrational frequency patterns. Several investigators have proposed formulae to derive S_{eff} based on molecular properties.

Benson and co-workers have advocated the use of the molar vibrational heat capacity (C_{vib}) to estimate S_{eff} [see Golden et al. (1971)]:

$$S_{eff} = \frac{C_{vib}}{R} . \tag{A-3}$$

C_{vib} may be estimated from tabulated values of Cp, the total heat capacity at constant pressure, by assuming that each translational and rotational degree of freedom contributes 1/2 R to the total (i.e., $C_{vib} = Cp - 4R$). Alternately, the molecular vibrational modes can be approximated as harmonic oscillators and C_{vib} computed using the statistical mechanic formula:

$$C_{vib} = \sum_{i=1}^{S} \frac{R\, x_i^2 \exp(-x_i)}{[1 - \exp(-x_i)]^2} , \tag{A-4}$$

where $x_i = h\upsilon_i/RT$, υ_i are the fundamental vibrational frequencies of the molecule, and the summation is taken over all of the (3N-6) normal harmonic oscillators (degenerate modes contribute identical terms to the summation). When υ_i are in units of cm^{-1} (see Table A-1), $x_i = 1.4388\ \upsilon_i/T$.

Use of the empirical rule given in Eq. (A-3) with classical RRK theory has been demonstrated [Golden et al. (1971) and Skinner and Rabinovitch (1972)] to predict approximately correct unimolecular fall-off curves for a wide variety of thermal reactions, provided k_∞ is greater than about $10^{-4}\ s^{-1}$.

An alternative formulation, used by Troe and co-workers [Troe and Wagner (1967), Glanzer and Troe (1972), Troe (1975)], is to estimate S_{eff} from the analogous statistical mechanical approximation for the (harmonic oscillator) vibrational internal energy (U_{vib}):

$$S_{eff} = \frac{E_{vib}}{RT} \sim \sum_{i=1}^{S} \frac{x_i}{\exp(x_i) - 1} \; . \qquad \text{(A-5)}$$

Figure A-3 illustrates a simple program, written in BASICA for the IBM PC, to compute S_{eff} based on the formulae given in Eqs. (A-4) and (A-5); a sample CRT screen output from execution of this program (for UF_6 at 1300 K) is given in Fig. A-4. Schug and Wagner (1977) report estimating S_{eff} for UF_6 at 1300 K to be 12.4, indicating that they used Troe formulation [see Eq. (A-5)] to help parameterize their version of the Kassel theory model.

In Table A-2, we compare the predicted values for S_{eff} [as defined in Eqs. (A-4) and (A-5)] with the value obtained by empirical fit (S_{eff} as an adjustable parameter, using RRK.BAS) for several compounds for which reliable experimental data or "sophisticated" theoretical predictions are available. Several points are noteworthy. First, within the sometimes considerable scatter of the experimental data, S_{eff} as a fitted parameter for a given reactant does not appear to change significantly over a considerable temperature range. Secondly, the predicted values for S_{eff} using heat-capacity-based formulae [Eq. (A-4)] are generally close in magnitude to the values obtained by empirical fit to the data, especially for higher temperatures, as has been previously observed by other investigators [Golden et al. (1971), Skinner and Rabinovitch (1972), and Schranz et al. (1982)]. In contrast, values for S_{eff} predicted by the Troe formula [Eq. (A-5)] are consistently too low for accurate predictions of unimolecular rates using the classical RRK model as given in Fig. A-1.

In Table A-2, the pressure-dependent data for cyclopropane, as reported by Barnard et al. (1974) and Lewis et al. (1978), were obtained using the shock-tube technique, with argon or helium as the propellant and bath gas. The Barnard et al. data were "corrected" to the corresponding self-medium values using the relative collision efficiencies reported by Snowden et al. (see previous discussion on parameterization of λ). Lewis et al. (1978) estimate a relative collision efficiency of ~0.04 in argon diluent over the temperature range of ~ 1000-1200 K.

RRK PARAMETERIZATION FOR GAS-PHASE THERMAL DISSOCIATION OF UF_6

As indicated in the main text, the comparative rate data derived from the laser-powered homogeneous pyrolysis experiment, with effective

```
10    OPTION BASE 1
20    PRINT"Estimate Seff=Cvib/R (Benson) and Seff=Uvib/kt (Troe)"
30    INPUT"number of fundamental harmonic oscillators=";N
40    DIM V(100),G(100),CV(100),FT(100),UV(100)
50    FOR L=1 TO N
60    INPUT"v(cm-1)=";V(L)
70    INPUT"degeneracy="(L)
80    NEXT L
90    INPUT"T(K)=";T
100   SM=0
110   SSM=0
120   FOR L=1 TO N
130   FT(L)=1.4388*V(L)/T
140   NU=1.987*EXP(-FT(L))*FT(L)*FT(L)
150   ND=(1-EXP(-FT(L)))^2
160   CV(L)=NU/ND
170   SF=CV(L)*G(L)
180   SM=SF+SM
190   SSF=SM/1.987
200   UV(L)=FT(L)/(EXP(FT(L))-1)
210   GUV=UV(L)*G(L)
220   SSM=GUV+SSM
230   NEXT L
240   PRINT"Cvib =";SM
250   SSF=SM/1.987
260   PRINT"Cvib/R =";SSF
270   PRINT "Uvib/kT =";SSM
280   GOTO90
```

Fig. A-3. Listing of program to compute S_{eff}(T) using harmonic oscillator frequency.

```
RUN
Estimate Seff=Cvib/R (Benson) and Seff=Uvib/kt (Troe)
number of fundamental harmonic oscillators=? 6
v(cm-1)=? 667
degeneracy=? 1
v(cm-1)=? 534
degeneracy=? 2
v(cm-1)=? 626
degeneracy=? 3
v(cm-1)=? 186
degeneracy=? 3
v(cm-1)=? 200
degeneracy=? 3
v(cm-1)=? 143
degeneracy=? 3
T(K)=? 1300
Cvib = 29.31294
Cvib/R = 14.75236
Uvib/kT = 12.37343
T(K)=?
```

Fig. A-4. Sample screen output from execution of Fig. A-3 example for UF$_6$ reactant at 1300 K.

Table A-2. Estimates of RRK parameters for selected reactant molecules

Reactant	Diluent	Data source	T(K)	Empirical fit (RRK,BAS):[a] λ	S_{eff}	$S \equiv C_{vib}/R$[b]	$S_{eff} \equiv E_{vib}/RT$[c]
Cyclopropane	Self	Yau and Pritchard (1978)	763.2	$\equiv 1$	13.8 ± 0.5	11.3	4.84
Cyclopropane	Self	Chambers and Kistiakowski (1934)	777.2	$\equiv 1$	13.7 ± 0.3	11.5	4.96
Cyclopropane	Self (Theory)[d]	Barnard et al. (1974)	800	$\equiv 1$	~13.9	11.7	5.15
Cyclopropane	Self	Furue and Pacey	897	$\equiv 1$	14.0 ± 0.2	12.8	5.92
Cyclopropane	Self (Theory)[d]	Barnard et al. (1974)	1100	$\equiv 1$	~14.6	14.5	7.35
Cyclopropane	Argon	Lewis et al. (1981)	1100	~0.04	~14.3	14.5	7.35
Cyclopropane	Self (Theory)[d]	Barnard et al. (1974)	1400	$\equiv 1$	~15.2	16.3	9.09
Ethyl Chloride	Self	Holbrook and Marsh (1967)	675	$\equiv 1$	11.8 ± 1.6	9.06	4.17
Ethyl Chloride	Self	Heydtmann et al. (1975)	754.7	$\equiv 1$	12.0 ± 0.3	9.92	4.73
Ethyl Chloride	Self	Holbrook and Marsh (1967)	767	$\equiv 1$	11.7 ± 0.6	10.0	4.82
Ethyl Chloride	Self	Holbrook and Marsh (1967)	794	$\equiv 1$	12.2 ± 0.4	10.3	5.00
Ethyl Chloride	Self	Blades et al. (1962)	922.5	$\equiv 1$	~12.4	11.4	5.82
Uranium Hexafluoride	Argon	Schug and Wagner (1977)	1300	0.05 ± 0.01	$\equiv$ 14.75	14.75	12.4
			1300	0.33 ± 0.06	$\equiv$ 12.4	14.75	12.4

[a] Computed with use of the program listed in Fig. A-1, the physical parameters listed in Table A-1, and the following values for the high-pressure limiting rate (k_∞):

$k_\infty(c\text{-}C_3H_6) = 1.48E15 \exp(-65{,}000/RT)$

$k_\infty(C_2H_5Cl) = 1.07E14 \exp(-58{,}430/RT)$

$k_\infty((UF_6) = 1.1E16 \exp(-67{,}760/RT)$

[b] See Eq. (A-4).

[c] See Eq. (A-5).

[d] Data are for reactant in Ar diluent "corrected" to self-medium using various theoretical treatments.

reaction temperature and "dwell time" as confounded parameters, are not readily amenable to interpretation in terms of "true" pressure dependency. Currently, the most complete pressure-dependent rate data are those reported by Schug and Wagner (1977) for UF_6 in argon diluent; data from their investigation are summarized in Table A-3. Schug and Wagner do not fully describe their selection of parameters but indicate that they used Kassel theory to extrapolate their data to the high-pressure limit. As suggested by Oref and Rabinovitch (1968), we have applied an empirical extrapolation procedure (1/k vs $[M]^{-0.5}$) to data summarized in Table A-3 to obtain a "preferred" expression for the rate at the high-pressure limit (see Fig. A-5):

$$k_\infty = 1.1E16\ \exp(-67{,}760/RT)\ s^{-1} \qquad (9)$$

Table A-3. Unimolecular reaction rate constants for UF_6 in argon medium
[Data from Schug and Wagner (1977)]

[Ar], mol/cm^{3b}	log k_u^{a} T = 1200 K	 T = 1300 K	 T = 1400 K
3E-6	2.794 ± 0.152	3.529 ± 0.134	4.148 ± 0.149
8E-6	2.962 ± 0.154	3.728 ± 0.128	4.393 ± 0.128
1.5E-5	3.074 ± 0.128	3.816 ± 0.126	4.482 ± 0.122
4E-6	3.233 ± 0.120	4.043 ± 0.122	4.736 ± 0.122

[a] Log k_u as read from Fig. 5 of Schug and Wagner text. Data points were apparently computed from pressure-dependent Arrhenius plots, and "I-bars" are assumed to represent the ±1σ error band for estimated rate as derived from the Arrhenius plot.

[b] P(torr) = 62361T(K)([M], mol/cm^3).

For our purposes, Eq. (9) of the main text is "preferred" for use with the RRK.BAS computational program for the following reasons, as will be indicated in later portions of this discussion: (1) when used with the data from Table A-3 and S_{eff} defined by C_{vib}/R, a "reasonable" value is estimated for the λ parameter for polyatomic reactant in argon medium (i.e., a value consistent with similar investigations in such medium); and (2) when the "strong collision" assumption is made for UF_6 in self-medium (i.e., λ = 1), the predicted rate fall-off (as k_u/k_∞) is in good agreement with sample calculations for UF_6 in self-medium using

DWG. NO. K/G-86-1453 (U)

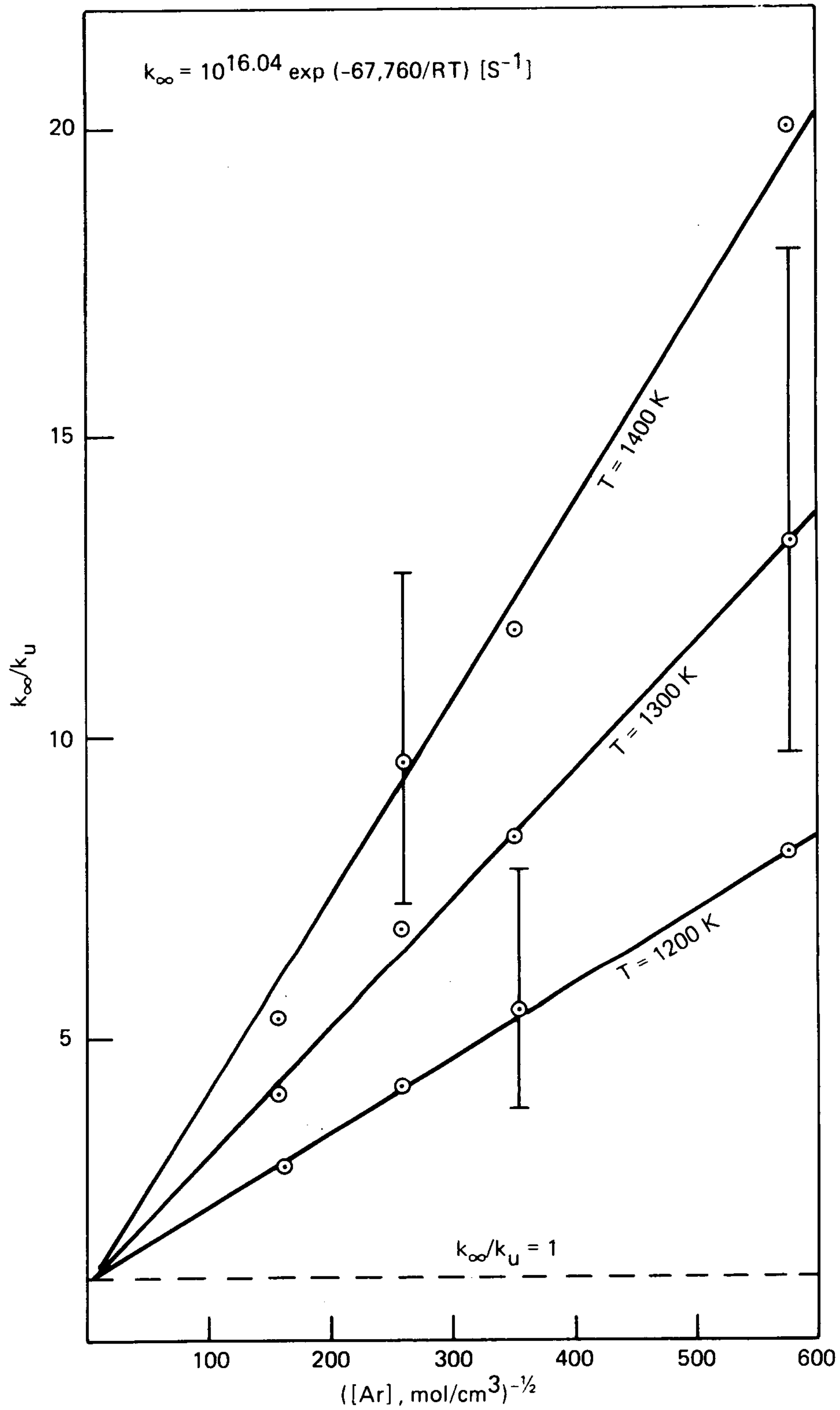

Fig. A-5. Data of Schug and Wagner (1977) plotted in an empirical manner to yield an estimate for the high-pressure limiting rate expression.

the more "sophisticated" Rice-Ramsperger-Kassel-Marcus (RRKM) quantum theory.

Since the data reported by Schug and Wagner are for rates measured in a bath comprised of a "weak" collision partner, modeling via classical RRK theory requires parameterization of both S_{eff} and λ, with additional "leverage" from the selected high-pressure Arrhenius parameters [see Furue and Pacey (1982)]. As shown in Figs. A-6 and A-7, essentially equivalent absolute rate predictions can be obtained using various permutations of parameters in the RRK model. From the data of Table A-2 and the previous discussion, we consider $S_{eff} = C_{vib}/R$ [see Eq. (A-3)] to represent an acceptable estimate for this parameter. Defining S_{eff} in this manner and using λ as the adjusted parameter, estimates for λ at 1300 K range from ~0.09 [using the high-pressure limiting Arrhenius parameters reported by Schug and Wagner [main text Eq. (8)] to ~0.05 (using the Arrhenius parameters empirically computed [Eq. (9)]. Using $S_{eff} = C_{vib}/R$ and Eq. (9) for the limiting high-pressure rate with all of the data listed in Table A-3, we obtain best root-mean-square fit for RRK $\lambda = 0.045$. These values for the λ term appear realistic compared with reported relative collision efficiencies for other comparable-sized polyatomic molecules in argon (e.g., $\beta_c \sim 0.04\text{-}0.07$ for cyclopropane in argon). Similarly, Schug and Wagner (1977) estimate $\beta_c = 0.03$ for UF_6 in argon.

In contrast, estimates for λ using $S_{eff} = U_{vib}/RT$ appear somewhat high (i.e., $\lambda = 0.2\text{-}0.3$). [The latter estimates are somewhat more consistent with the relative vibrational relaxation time constants for UF_6 in argon vs self-medium, as reported by Cravens et al. (1979); however, relatively efficient V-T relaxation does not, in general, indicate efficient deactivation in thermal unimolecular reactions.]

Lyman and Holland (unpublished results, May 1985) have applied RRKM quantum theory to UF_6 thermal dissociation, parameterized to the Schug and Wagner data. We have used sample calculations for UF_6 in self-medium by the more "sophisticated" (and computationally rigorous) RRKM theory to aid in the parameterization of the "simplified" RRK treatment--subject, of course, to the assumptions employed in the RRKM formulation regarding details of potential surfaces and intermolecular energy transfer processes [a similar parameterization procedure for the "simplified" theory, based on RRKM predictions, is advocated in Troe (1979)]. Agreement between classical RRK predictions (with $S_{eff} \equiv C_{vib}/R$) and RRKM theory is expected to be close for UF_6, provided the temperature is greater than about 740 K [i.e., $k_\infty > 1E\text{-}4$; see Golden et al. (1971)]. This is confirmed in Fig. A-8, in which the RRK predictions for UF_6 in self-medium are based on the "strong-collision" assumption (i.e., $\lambda = 1$) and the input parameters listed in Table A-4. These same parameters (with $\lambda \sim 0.05$) also adequately reproduce the original Schug and Wagner data for UF_6 in argon diluent, as shown in Fig. A-7.

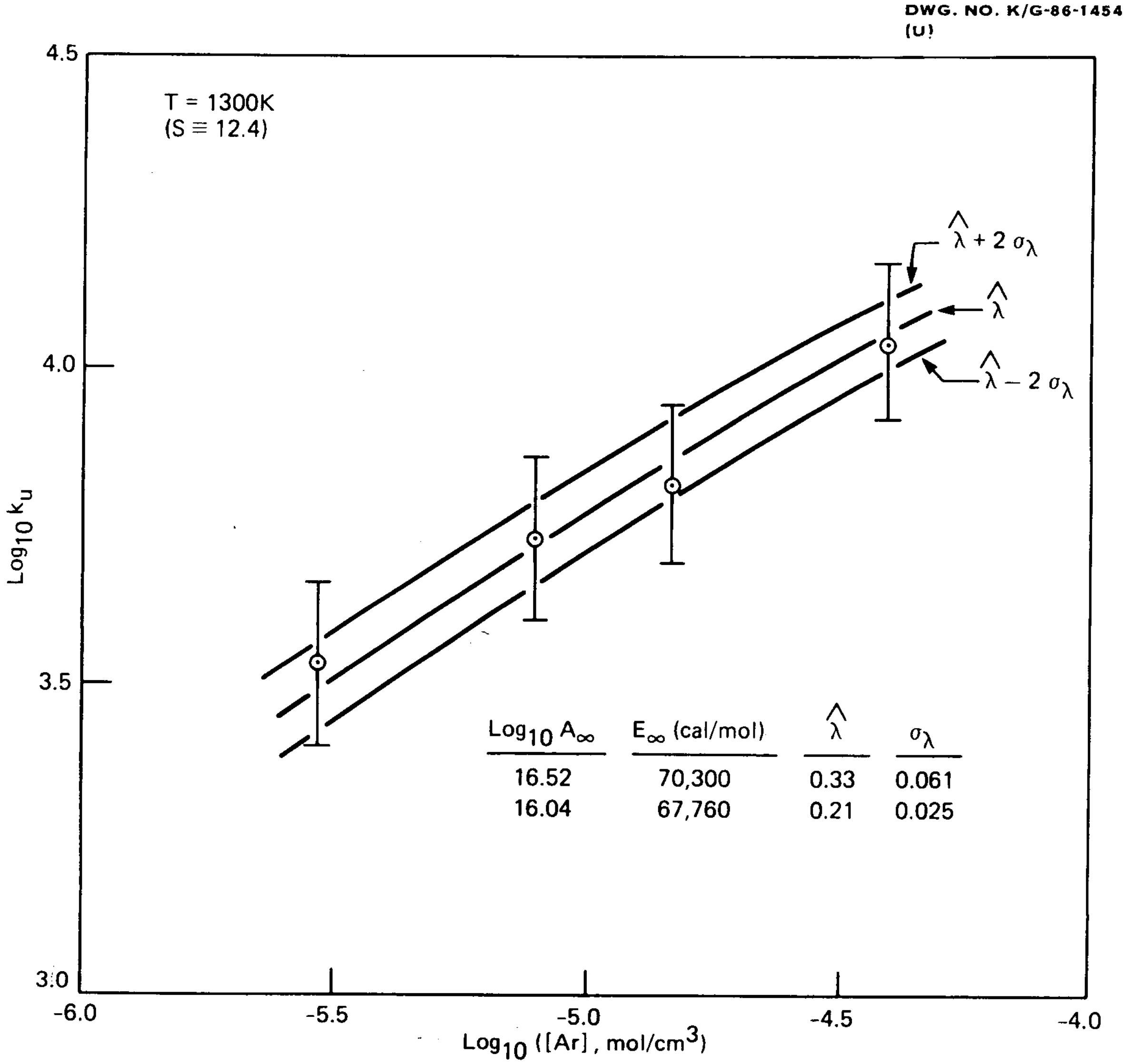

Fig. A-6. Data of Schug and Wagner (1977): RRK predictions using $S_{eff} = U_{vib}/RT$, with λ as the adjusted parameter.

DWG. NO. K/G-87-379
(U)

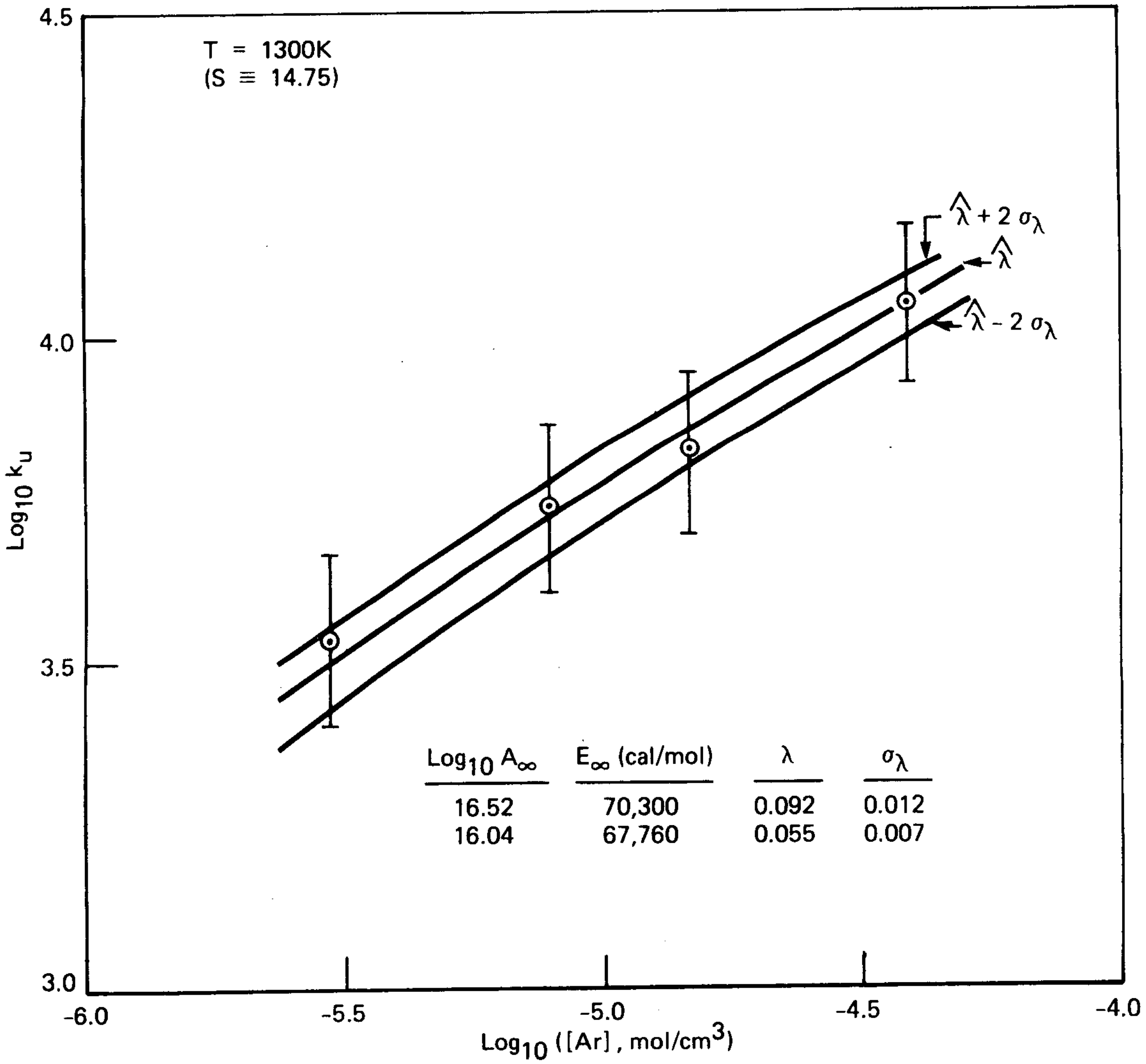

$\mathrm{Log}_{10}\,A_\infty$	E_∞ (cal/mol)	λ	σ_λ
16.52	70,300	0.092	0.012
16.04	67,760	0.055	0.007

Fig. A-7. Data of Schug and Wagner (1977): RRK Predictions using $S_{eff} = C_{vib}/R$, with λ as the adjusted parameter.

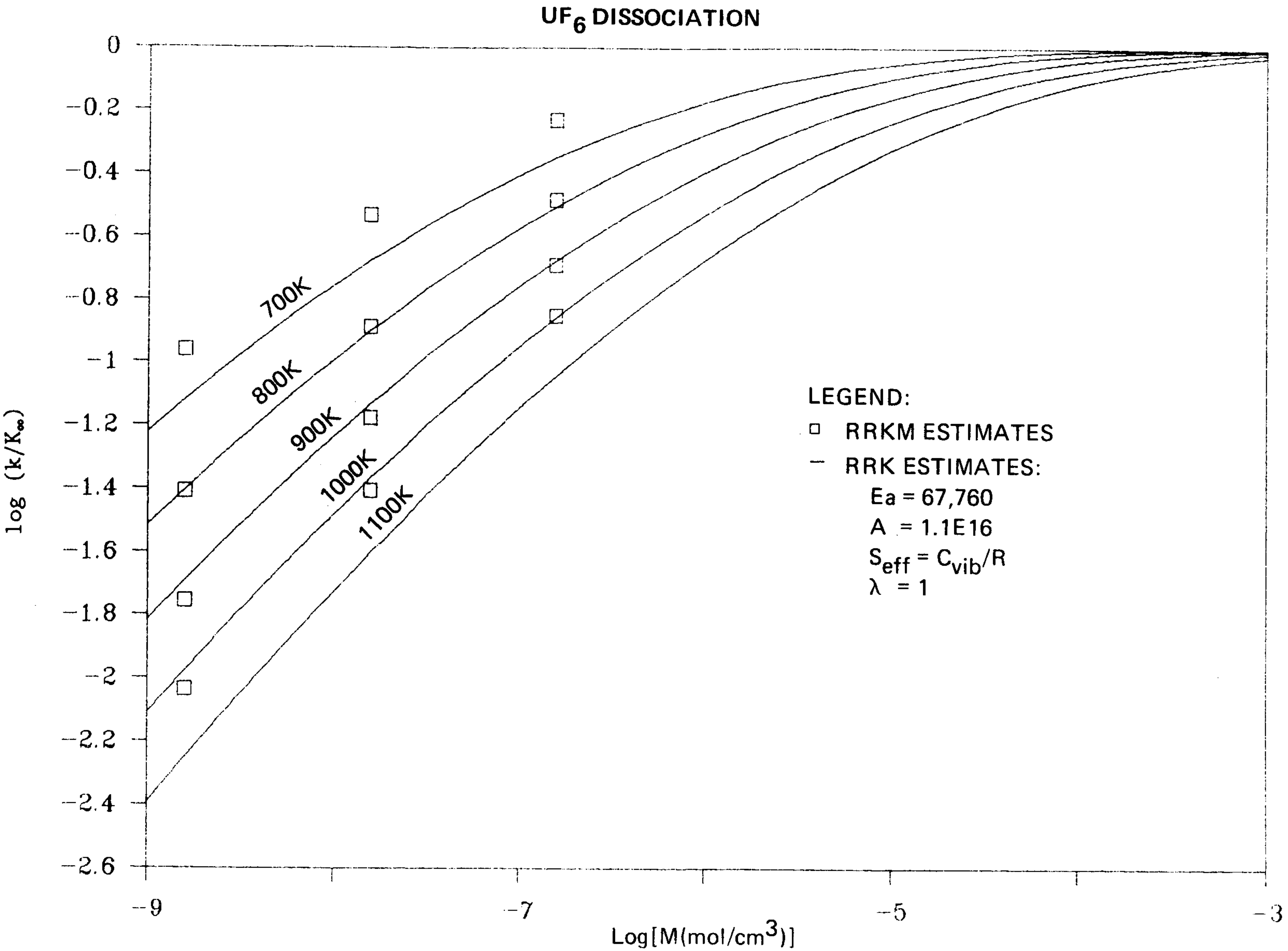

Fig. A-8. Gas-phase unimolecular reaction rate predictions for UF_6. Solid curves: RRK predictions, with $S_{eff} = C_{vib}/R$ and $\lambda = 1$. Symbols: RRKM predictions for T = 700, 800, 900, and 1000 K (Lyman and Holland, unpublished results, May 1985).

Table A-4. RRK.BAS: Selected parameters for predicting the gas-phase thermal dissociation rate for UF_6

Input parameter	Value selected	Text reference
Ea (cal/mol)	67760	Eq. (9)
Ao (1/s)	1.1E16	Eq. (9)
Reactant mass (amu)	352	Table A-1
Reactant diam. (Ang)	5.97	Table A-1
Diluent diam. (Ang)	(e.g., 3.54 for argon)	Table A-1
λ	1 (self-medium) 0.045 (argon diluent)	Fig. A-8 Fig. A-7
RRK S factor	C_{vib}/R	Eq. (A-3), Table A-3

DISTRIBUTION

Emory University
- M. Kaufman

Lawrence Livermore National Laboratory
- J. Z. Holtz
- J. A. Viecelli
- S. Stone

Los Alamos National Laboratory
- D. B. Fradkin
- R. Holland
- K. C. Kim
- J. L. Lyman
- W. H. McCulla (3)
- R. S. McDowell
- H. H. Watanabe

Martin Marietta Energy Systems, Inc.
- D. P. Armstrong
- E. J. Barber
- W. D. Bostick (5)
- J. T. Bradbury, III
- Central Research Library
- R. N. Compton
- Enrichment Technology Library
- D. E. Fain
- R. L. Fellows

Martin Marietta Energy Systems, Inc. (Cont.)
- R. L. Higgins
- W. S. Key
- J. J. Keyes, Jr.
- G. J. Kidd, Jr.
- C. E. Klots
- K. H. Lin
- F. C. Maienschein
- D. N. Mashburn
- J. R. Merriman
- S. H. Park
- J. R. Peterson
- F. G. Pin
- A. S. Quist (3)
- R. H. Reiner
- R. C. Riepe
- W. L. Roberts
- S. A. Sherrow
- K. D. Streetman
- A. J. Szady
- L. D. Trowbridge (3)
- D. A. Waters
- C. R. Weisbin
- W. R. Williams

SRI International
- D. M. Golden
- D. L. Hildenbrand